AEROSOL STABILILITY OF SEVERE ACUTE RESPIRATORY SYNDROME CORONAVIRUS 2

(SARS-CoV-2)

by

Trenton John Bushmaker

A thesis submitted in partial fulfillment
of the requirements for the degree

of

Master of Science

in

Microbiology and Immunology

MONTANA STATE UNIVERSITY
Bozeman, Montana

May 2022

DEDICATION

I dedicate this thesis to my beautiful wife Cara, my children Isla and Breccan, parents Julie and Bob, and my dog Bentley; who provided support and encouragement throughout my coursework at Montana State University. I love you.

ACKNOWLEDGEMENTS

I would like to show my immense gratitude to my co-advisors Dr. Raina K. Plowright and Dr. Vincent J. Munster for support on this project. Dr. Plowright has provided her gentle guidance while providing precision assessments during all stages of the writing process. I would like to express my sincere appreciation to Dr. Plowright for the profound mentorship, emotional support, and educational assistance. Dr. Munster has demonstrated the skillset required to bring the project to completion, all while providing the mentorship and avenues of support for my educational achievement. This work would've not been possible without their continuous advice, inspirations, and scientific merit.

It is my pleasure to expression my deep sense thankfulness for the experimental support provided by Myndi Holbrook, Dr. Dylan Morris, Dr. Amandine Gamble, Dr. Neeltje van Doremalen, and Dr. Kwe Claude Yinda. The achievement of the project was only obtained by their timely advice, scientific capabilities, and hard work during long days.

It has been my privilege to have Dr. Jayne Morrow and Dr. Heinz Feldmann as graduate committee members. Their scientific and personal feedback has been essential for my development; all while providing a kind ear and encouragement.

In final, I am extremely thankful for Dr. Munster and Dr. Feldmann for providing the patience, employment flexibility, and enthusiasm during my personal educational endeavors.

TABLE OF CONTENTS

LIST OF TABLES

Table Page

LIST OF FIGURES

Figure Page

ABSTRACT

The routes of transmission of the zoonotic pathogen severe acute respiratory syndrome coronavirus-2 (SARS-CoV-2) have been extensively studied to understand the spread at individual and population levels. Aerosol particles produced by infected individuals and the deposition patterns inhaled are known to affect the virulence of bioaerosol pathogens. Droplet nuclei particles (< 5 μm) aerosols typically deposit within the alveolar spaces of the lungs, whereas droplet (>5 μm) aerosols typically deposit within the nasopharyngeal and tracheobronchial regions of the respiratory tract. A few studies have evaluated pulmonary disease following droplet nuclei size particles of SARS-CoV-2 aerosol inhalation in African green monkeys and golden hamsters, concluding that both models have mild respiratory disease representative of human disease [1, 2] . More importantly, human participants with SARS-CoV-2 infections have been studied to look at the generation of particles during breathing, talking, and singing; the study concluded droplet nuclei particles accounted for 85% of the copies of virus produced and play a significant role in transmission [3]. However, the environmental persistence of the aerosolized droplet nuclei particles, and the likely role of environmental persistence in driving transmission, is unknown for SARS-CoV-2.

In these studies, we show the changing aerosol stability of SARS-CoV-2 during the supplanting waves of Variants of Concern (VOC). With the determination of viable viral particles characterized over time, we can make inferences about the role VOC and aerosol transmission have in driving population-level pathogen transmission. A secondary objective of these studies was to characterize the role those evolving mutations have had on viral entry and aerosol durability. Our work suggests that aerosol stability may be important in driving some population-level phenomena (e.g., indoor transmission, including superspreader events) but given the short infected-to-naïve transmission transit time, the variation in the duration of aerosol stability among VOCs may not explain the difference in transmission rates of VOCs. This data will be useful for assessing the future evolution of aerosol transmission of SARS-CoV-2.

CHAPTER ONE

INTRODUCTION

The seemingly perpetual coronavirus disease 2019 (COVID-19) pandemic was triggered by the novel human pathogen severe acute respiratory syndrome coronavirus 2 (SARS-CoV-2) in the genus of *Betacoronavirus*. The subgenus *Sarbecovirus* contains another human pathogen called severe acute respiratory syndrome coronavirus (SARS-CoV, called here SARS-CoV-1), which emerged in late 2002 - 2003. Another notable human *Betacoronavirus*, Middle East respiratory syndrome coronavirus (MERS-CoV), is in a relatable subgenus *Merbecovirus* [4]. These viruses have provided the essential initial experimental templates for our stability studies.

Since the emergence of SARS-CoV-1 this virus has caused nearly 800 deaths and >8,000 confirmed cases. The virus spread to 26 countries, highlighting the threat posed by emerging coronaviruses to public health. During these initial cases, epidemiological studies of SARS-CoV-1 identified the aerosol and fomite transmission potential, during the investigation of the well-known Hotel Metropole superspreader event [5].

In 2012, MERS-CoV was identified in human patients and had been traced back to origins in dromedary camels. Human infection with MERS-CoV has reached over 2,500 cases with a mortality rate of ~35% and has spread to 27 countries with multiple camel-to-human outbreaks [6, 7]. Epidemiologic evidence strongly supports evidence of human aerosol and fomite transmission in nosocomial and community settings with large superspreader events [8].

In light of this information, we looked at these two routes of transmission in relation to the emergence of different isolates and their associated mutations in the Spike(s) glycoprotein. In the aerosol section of the experiment, the rotating Goldberg drum apparatus (Figure 1.1) (Biaera

Technologies) was used to keep the aerosol suspended to avoid any gravitational settling (deposition) resulting in large physical loss [9]. The apparatus can be used at a set relative humidity (RH%) to simulate desiccation of the particle. Temperature conditions are limited by ambient air space around the unit. For the MERS-CoV study, the RH% was 60-70% and temperature was constant at 21°C. In addition, the system's rotating drum is enclosed to prevent any further UV degradation of the particle composition encasing the virus or the virus itself. We used controlled laboratory reagents to retain the physiochemistry of the particles; whereas we avoided using body fluids (e.g., mucus) as a vehicle to mimic environmental persistence because of inconsistent antiviral properties that would hamper isolate comparisons. With the use of naturally occurring "house" air from the building environment, concerns of antiviral effects from H_2O_2 concentrations were eliminated and should not lead to inconsistencies in environmental conditions. In conclusion, the MERS-CoV isolates might have similar environmental stability profiles and any individual variation can influence this phenotype; underscoring the need for continued global viral surveillance and assessment of the phenotypic properties of the MERS-CoV isolates [10].

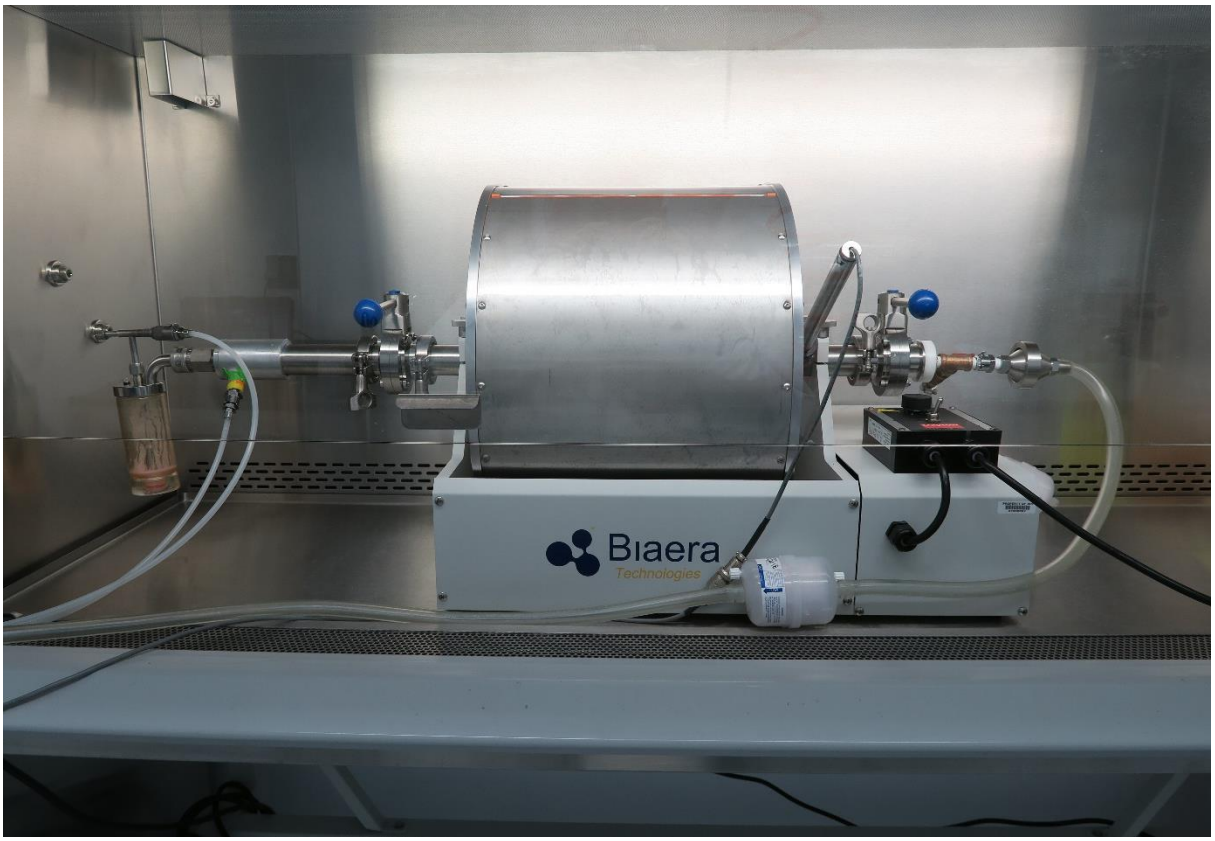

FIGURE 1.1 – Goldberg drum apparatus. The rotational motion of the drum section is used to keep the aerosol in suspension, with internal baffles, for the duration of the experiment.

The MERS-CoV study was an important analysis for different isolates in relation to aerosol stability for coronaviruses, setting up comparison studies for future respiratory coronavirus outbreaks. While the MERS-CoV manuscript was in preparation; SARS-CoV-2 emerged. We quickly utilized the aerosol stability framework to assess the comparative stability with regards to MERS-CoV. No significant difference was observed between MERS-CoV and SARS-CoV-2 in the study, suggesting broader environmental similarities between viruses with similar composition.

Although the threat of coronaviruses to public health was not widely appreciated

prior to SARS-CoV-1; the yearly outbreaks of MERS-CoV had provided a training ground for the SARS-CoV-2 pandemic. Epidemiological models, ecological surveillance, laboratory transmission studies, vaccine development, and functional aerosol experiments had all been conducted on MERS-CoV. Epidemiologists were able to study superspreader events and the role of comorbidities in disease. In SARS-CoV-2 the role of aging and comorbidities impact on disease outcomes was mirrored [8, 11-14]. Ecological surveillance was important to examine the role of camels in zoonotic transmission of MERS-CoV; this work has been important for SARS-CoV-2 in regard to origin identification [15-17]. In MERS-CoV, transmission studies were important to understand zoonotic and community transmission; in SARS-CoV-2 transmission studies were vital to understand the primary route of aerosol transmission [10, 18, 19]. Vaccine development for MERS-CoV lead to an established pipeline for the development of the Oxford/AstraZeneca (ChAdOx1-S [recombinant]) COVID-19 vaccine, and with subsequent vaccination of 2.5 billion people in over 170 countries [20, 21].

With the effort we put forth into understanding MERS-CoV, we were able to use the developed fomite and aerosol transmission experiments to pivot working towards SARS-CoV-2. Fomite experiments had been established during the 2014 - 2015 Ebola virus outbreaks, MERS-CoV epidemic, and continued for comparison between SARS-CoV-1 vs. SARS-CoV-2 in Chapter 2 [10, 22, 23]. These fomite experiments have provided key information for clinical settings during outbreak situations.

The 2014 Ebola outbreak in West Africa, lay the foundation for research focused on understanding viral stability and transmission which led to an increase in understanding on: persistence in body fluids (e.g., semen and blood), persistence in carcasses, and persistence in

aerosols [24-26]. We moved to include more natural mucosal fluids into the stability studies, using human mucus and sputum, to understand the environmental effects on the stability of SARS-CoV-2 [27]. Additionally, and most importantly, the foundation of aerosol stability studies for Ebola and MERS-CoV provided the rapid pivot to SARS-CoV-2 [10, 15].

With the development of experimental assays on the environmental stability of Ebola virus, SARS-CoV-1, and MERS-CoV, we lay the foundation of a rapid phenotypic assessment of essential viral properties related to human-to-human transmission. We were able to observe the underlying role that SARS-CoV-2 stability has on the COVID-19 pandemic. In the next two chapters, we were able to provide imperative stability data during the successional waves of variants during the COVID-19 pandemic.

CHAPTER TWO

AEROSOL AND SURFACE STABILITY OF SARS-CoV-2 AS COMPARED WITH SARS-CoV-1

Contribution of Authors and Co-Authors

Manuscript in Chapter 2

Author: Neeltje van Doremalen *

Contributions: Conceptualization, writing, resources, and visualization.

Author: Trenton Bushmaker *

Contributions: Conceptualization, methodology, data curation, and writing.

Author: Dylan H. Morris *

Contributions: Conceptualization, data curation, visualization, and writing.

Co-Author: Myndi G. Holbrook

Contributions: Methodology.

Co-Author: Amandine Gamble

Contributions: Data curation and visualization.

Co-Author: Brandi N. Williamson

Contributions: Resources.

Co-Author: Azaibi Tamin

Contributions: Resources.

Co-Author: Jennifer L. Harcourt

Contributions: Resources.

Co-Author: Natalie J. Thornburg

Contributions: Resources.

Co-Author: Susan I. Gerber

Contributions: Resources.

Co-Author: James O. Lloyd-Smith

Contributions: Conceptualization, writing, and supervision.

Co-Author: Emmie de Wit

Contributions: Conceptualization, supervision and resources.

Co-Author: Vincent J. Munster

Contributions: Conceptualization, writing, supervision and resources.

NOTE: * These authors contributed equally to this article

Manuscript Information

Neeltje van Doremalen, Trenton Bushmaker, Dylan H. Morris, Myndi G. Holbrook, Amandine Gamble, Brandi N. Williamson, Azaibi Tamin, Jennifer L. Harcourt, Natalie J. Thornburg, Susan I. Gerber, James O. Lloyd-Smith, Emmie de Wit, and Vincent J. Munster

New England Journal of Medicine

Status of Manuscript:
____ Prepared for submission to a peer-reviewed journal
____ Officially submitted to a peer-reviewed journal
____ Accepted by a peer-reviewed journal
_X_ Published in a peer-reviewed journal

New England Journal of Medicine
Published: March 17, 2020
Issue: April 16, 2020
N Engl J Med 2020; 382:1564-1567
DOI: 10.1056/NEJMc2004973

The NEW ENGLAND JOURNAL of MEDICINE

CORRESPONDENCE

Aerosol and Surface Stability of SARS-CoV-2 as Compared with SARS-CoV-1

TO THE EDITOR: A novel human coronavirus that is now named severe acute respiratory syndrome coronavirus 2 (SARS-CoV-2) (formerly called HCoV-19) emerged in Wuhan, China, in late 2019 and is now causing a pandemic.[1] We analyzed the aerosol and surface stability of SARS-CoV-2 and compared it with SARS-CoV-1, the most closely related human coronavirus.[2]

We evaluated the stability of SARS-CoV-2 and SARS-CoV-1 in aerosols and on various surfaces and estimated their decay rates using a Bayesian regression model (see the Methods section in the Supplementary Appendix, available with the full text of this letter at NEJM.org). SARS-CoV-2 nCoV-WA1-2020 (MN985325.1) and SARS-CoV-1 Tor2 (AY274119.3) were the strains used. Aerosols (<5 μm) containing SARS-CoV-2 ($10^{5.25}$ 50% tissue-culture infectious dose [$TCID_{50}$] per milliliter) or SARS-CoV-1 ($10^{6.75-7.00}$ $TCID_{50}$ per milliliter) were generated with the use of a three-jet Collison nebulizer and fed into a Goldberg drum to create an aerosolized environment. The inoculum resulted in cycle-threshold values between 20 and 22, similar to those observed in samples obtained from the upper and lower respiratory tract in humans.

Our data consisted of 10 experimental conditions involving two viruses (SARS-CoV-2 and SARS-CoV-1) in five environmental conditions (aerosols, plastic, stainless steel, copper, and cardboard). All experimental measurements are reported as means across three replicates.

SARS-CoV-2 remained viable in aerosols throughout the duration of our experiment (3 hours), with a reduction in infectious titer from $10^{3.5}$ to $10^{2.7}$ $TCID_{50}$ per liter of air. This reduction was similar to that observed with SARS-CoV-1, from $10^{4.3}$ to $10^{3.5}$ $TCID_{50}$ per milliliter (Fig. 1A).

SARS-CoV-2 was more stable on plastic and stainless steel than on copper and cardboard, and viable virus was detected up to 72 hours after application to these surfaces (Fig. 1A), although the virus titer was greatly reduced (from $10^{3.7}$ to $10^{0.6}$ $TCID_{50}$ per milliliter of medium after 72 hours on plastic and from $10^{3.7}$ to $10^{0.6}$ $TCID_{50}$ per milliliter after 48 hours on stainless steel). The stability kinetics of SARS-CoV-1 were similar (from $10^{3.4}$ to $10^{0.7}$ $TCID_{50}$ per milliliter after 72 hours on plastic and from $10^{3.6}$ to $10^{0.6}$ $TCID_{50}$ per milliliter after 48 hours on stainless steel). On copper, no viable SARS-CoV-2 was measured after 4 hours and no viable SARS-CoV-1 was measured after 8 hours. On cardboard, no viable SARS-CoV-2 was measured after 24 hours and no viable SARS-CoV-1 was measured after 8 hours (Fig. 1A).

THIS WEEK'S LETTERS

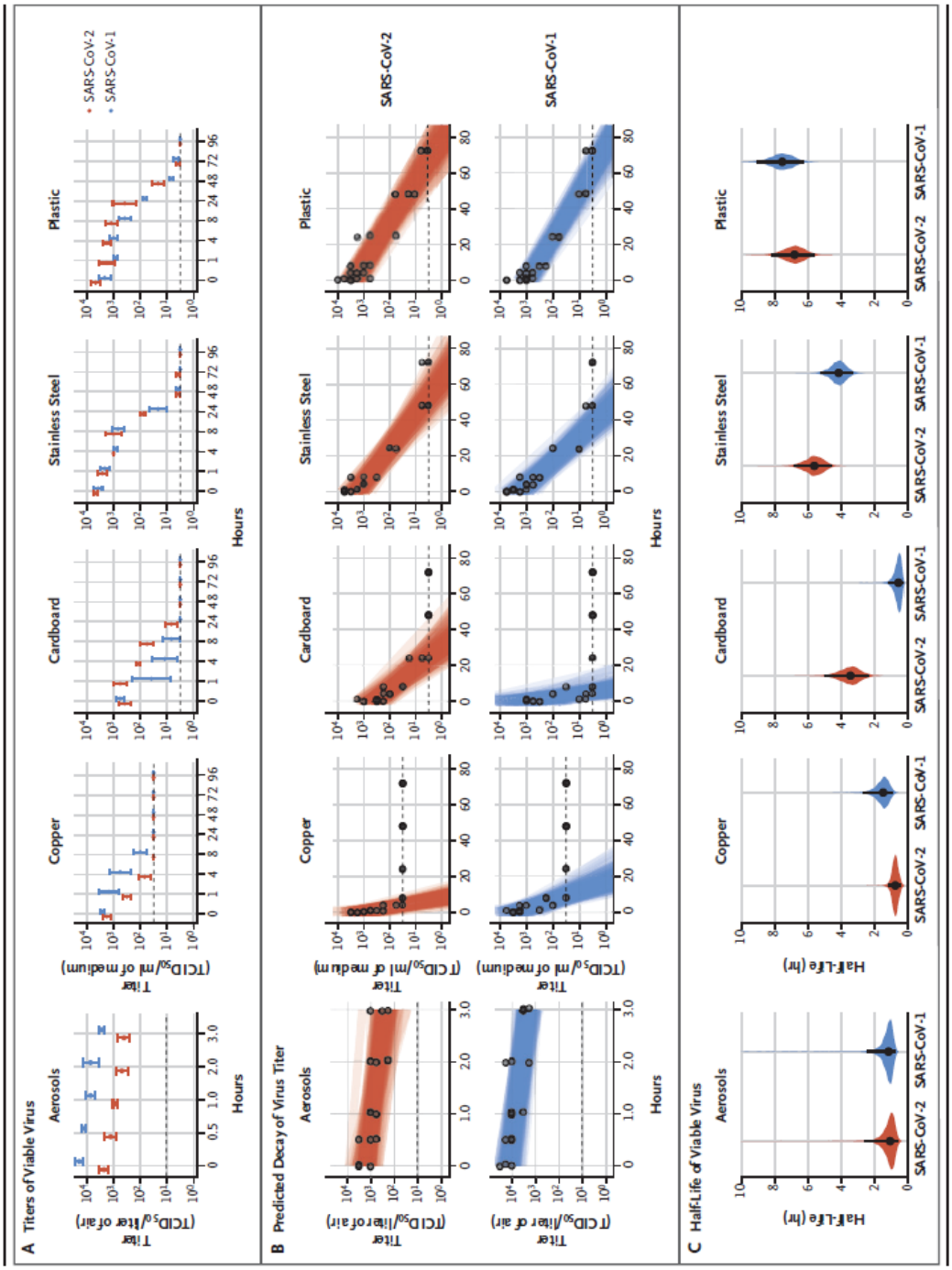

Figure 1 (previous page). Viability of SARS-CoV-1 and SARS-CoV-2 in Aerosols and on Various Surfaces. As shown in Panel A, the titer of aerosolized viable virus is expressed in 50% tissue-culture infectious dose ($TCID_{50}$) per liter of air. Viruses were applied to copper, cardboard, stainless steel, and plastic maintained at 21 to 23°C and 40% relative humidity over 7 days. The titer of viable virus is expressed as $TCID_{50}$ per milliliter of collection medium. All samples were quantified by end-point titration on Vero E6 cells. Plots show the means and standard errors (I bars) across three replicates. As shown in Panel B, regression plots indicate the predicted decay of virus titer over time; the titer is plotted on a logarithmic scale. Points show measured titers and are slightly jittered (i.e., their horizontal positions are modified by a small random amount to reduce overlap) along the time axis to avoid overplotting. Lines are random draws from the joint posterior distribution of the exponential decay rate (negative of the slope) and intercept (initial virus titer) to show the range of possible decay patterns for each experimental condition. There were 150 lines per panel, including 50 lines from each plotted replicate. As shown in Panel C, violin plots indicate posterior distribution for the half-life of viable virus based on the estimated exponential decay rates of the virus titer. The dots indicate the posterior median estimates, and the black lines indicate a 95% credible interval. Experimental conditions are ordered according to the posterior median half-life of SARS-CoV-2. The dashed lines indicate the limit of detection, which was $3.33\times10^{0.5}$ $TCID_{50}$ per liter of air for aerosols, $10^{0.5}$ $TCID_{50}$ per milliliter of medium for plastic, steel, and cardboard, and $10^{1.5}$ $TCID_{50}$ per milliliter of medium for copper.

Both viruses had an exponential decay in virus titer across all experimental conditions, as indicated by a linear decrease in the $\log_{10}TCID_{50}$ per liter of air or milliliter of medium over time (Fig. 1B). The half-lives of SARS-CoV-2 and SARS-CoV-1 were similar in aerosols, with median estimates of approximately 1.1 to 1.2 hours and 95% credible intervals of 0.64 to 2.64 for SARS-CoV-2 and 0.78 to 2.43 for SARS-CoV-1 (Fig. 1C, and Table S1 in the Supplementary Appendix). The half-lives of the two viruses were also similar on copper. On cardboard, the half-life of SARS-CoV-2 was longer than that of SARS-CoV-1. The longest viability of both viruses was on stainless steel and plastic; the estimated median half-life of SARS-CoV-2 was approximately 5.6 hours on stainless steel and 6.8 hours on plastic (Fig. 1C). Estimated differences in the half-lives of the two viruses were small except for those on cardboard (Fig. 1C). Individual replicate data were noticeably "noisier" (i.e., there was more variation in the experiment, resulting in a larger standard error) for cardboard than for other surfaces (Fig. S1 through S5), so we advise caution in interpreting this result.

We found that the stability of SARS-CoV-2 was similar to that of SARS-CoV-1 under the experimental circumstances tested. This indicates that differences in the epidemiologic characteristics of these viruses probably arise from other factors, including high viral loads in the upper respiratory tract and the potential for persons infected with SARS-CoV-2 to shed and transmit the virus while asymptomatic.[3,4] Our results indicate that aerosol and fomite transmission of SARS-CoV-2 is plausible, since the virus can remain viable and infectious in aerosols for hours and on surfaces up to days (depending on the inoculum shed). These findings echo those with SARS-CoV-1, in which these forms of transmission were associated with nosocomial spread and super-spreading events,[5] and they provide information for pandemic mitigation efforts.

Neeltje van Doremalen, Ph.D.
Trenton Bushmaker, B.Sc.
National Institute of Allergy and Infectious Diseases
Hamilton, MT

Dylan H. Morris, M.Phil.
Princeton University
Princeton, NJ

Myndi G. Holbrook, B.Sc.
National Institute of Allergy and Infectious Diseases
Hamilton, MT

Amandine Gamble, Ph.D.
University of California, Los Angeles
Los Angeles, CA

Brandi N. Williamson, M.P.H.
National Institute of Allergy and Infectious Diseases
Hamilton, MT

Azaibi Tamin, Ph.D.
Jennifer L. Harcourt, Ph.D.
Natalie J. Thornburg, Ph.D.
Susan I. Gerber, M.D.
Centers for Disease Control and Prevention
Atlanta, GA

James O. Lloyd-Smith, Ph.D.
University of California, Los Angeles
Los Angeles, CA
Bethesda, MD

Emmie de Wit, Ph.D.
Vincent J. Munster, Ph.D.
National Institute of Allergy and Infectious Diseases
Hamilton, MT
vincent.munster@nih.gov

Dr. van Doremalen, Mr. Bushmaker, and Mr. Morris contributed equally to this letter.

The findings and conclusions in this letter are those of the authors and do not necessarily represent the official position of the Centers for Disease Control and Prevention (CDC). Names of specific vendors, manufacturers, or products are included for public health and informational purposes; inclusion does not imply endorsement of the vendors, manufacturers, or products by the CDC or the Department of Health and Human Services.

Supported by the Intramural Research Program of the National Institute of Allergy and Infectious Diseases, National Institutes of Health, and by contracts from the Defense Advanced Research Projects Agency (DARPA PREEMPT No. D18AC00031, to Drs. Lloyd-Smith and Gamble), from the National Science Foundation (DEB-1557022, to Dr. Lloyd-Smith), and from the Strategic Environmental Research and Development Program of the Department of Defense (SERDP, RC-2635, to Dr. Lloyd-Smith).

Disclosure forms provided by the authors are available with the full text of this letter at NEJM.org.

This letter was published on March 17, 2020, at NEJM.org.

1. Coronavirus disease (COVID-2019) situation reports. Geneva: World Health Organization, 2020 (https://www.who.int/emergencies/diseases/novel-coronavirus-2019/situation-reports/).
2. Wu A, Peng Y, Huang B, et al. Genome composition and divergence of the novel coronavirus (2019-nCoV) originating in China. Cell Host Microbe 2020;27:325-8.
3. Bai Y, Yao L, Wei T, et al. Presumed asymptomatic carrier transmission of COVID-19. JAMA 2020 February 21 (Epub ahead of print).
4. Zou L, Ruan F, Huang M, et al. SARS-CoV-2 viral load in upper respiratory specimens of infected patients. N Engl J Med 2020;382:1177-9.
5. Chen YC, Huang LM, Chan CC, et al. SARS in hospital emergency room. Emerg Infect Dis 2004;10:782-8.

DOI: 10.1056/NEJMc2004973

Supplementary Appendix

This appendix has been provided by the authors to give readers additional information about their work.

Supplement to: van Doremalen N, Bushmaker T, Morris DH, et al. Aerosol and surface stability of SARS-CoV-2 as compared with SARS-CoV-1. N Engl J Med 2020;382:1564-7. DOI: 10.1056/NEJMc2004973

Table of contents:

Supplemental methods

Laboratory experiments

Viruses and titration

HCoV-19 nCoV-WA1-2020 (MN985325.1) (Holshue et al., 2020) and SARS-CoV-1 Tor2 (AY274119.3) (Marra et al., 2003) were the strains used in our comparison. Viable virus in all surface and aerosol samples was quantified by end-point titration on Vero E6 cells as described previously (van Doremalen et al., 2013).

Virus stability in aerosols

Virus stability in aerosols was determined as described previously at 65% relative humidity (RH) and 21-23°C (Fischer et al., 2016). In short, aerosols (<5 µm) containing HCoV-19 ($10^{5.25}$ $TCID_{50}$/mL) or SARS-CoV-1 ($10^{6.75-7}$ TCID50/mL) were generated using a 3-jet Collison nebulizer and fed into a Goldberg drum to create an aerosolized environment. Aerosols were maintained in the Goldberg drum and samples were collected at 0, 30, 60, 120 and 180 minutes post-aerosolization on a 47mm gelatin filter (Sartorius). Filters were dissolved in 10 mL of DMEM containing 10% FBS. Three replicate experiments were performed.

Virus stability on surfaces

Surface stability was evaluated on plastic (polypropylene, ePlastics), AISI 304 alloy stainless steel (Metal Remnants), copper (99.9%) (Metal Remnants) and cardboard (local supplier) representing a variety of household and hospital situations and was performed as described previously at 40% RH and 21-23°C using an inoculum of 10^5 $TCID_{50}$/mL (van Doremalen et al., 2013). This inoculum resulted in cycle-threshold values (Ct) between 20 and 22 similar to those observed in samples from human upper and lower respiratory tract (Zou et al., 2020). In short, 50 µl of virus was deposited on the surface and recovered at predefined time-points by adding 1 mL of DMEM. Stability on cardboard was evaluated by depositing 50 µl of virus on the surface and recovering the inoculum by swabbing of the surface, the swab was deposited 1 mL of DMEM. Three replicate experiments were performed for each surface.

Statistical analyses

Bayesian regression model description

The durations of detectability depend on initial inoculum and sampling method, as expected. To evaluate the inherent stability of the viruses, we estimated the decay rates of viable virus titers using a Bayesian regression model. This modeling approach allowed us to account for differences in initial inoculum levels across replicates, as well as interval-censoring of titer data and other sources of experimental noise. The model yields estimates of posterior distributions of viral decay rates and half-lives in the various experimental conditions – that is, estimates of the range of plausible values for these parameters given our data, with an estimate of the overall uncertainty (Gelman et al., 2013).

In the model notation that follows, the symbol ~ denotes that a random variable is distributed according to the given distribution. Normal distributions are parametrized as Normal(mean, standard deviation). Positive-constrained normal distributions ("Half-Normal") are parametrized as Half-Normal(mode, standard deviation). We use <Distribution Name>CDF(x, parameters) to denote the cumulative distribution function of a probability distribution, so for example NormalCDF(5, 0, 1) is the value of the Normal(0, 1) cumulative distribution function at 5.

Our data consist of 10 experimental conditions: 2 viruses (HCoV-19 and SARS-CoV-1) by 5 environmental conditions (aerosols, plastic, stainless steel copper and cardboard). Each has three replicates, and multiple time-points for each replicate. We analyze the two viruses separately. For each, we denote by y_{ijk} the measured $\log_{10}$ titer in experimental condition i during replicate j at time-point k. To construct our likelihood function, we need to know the probability of observing a given $\log_{10}$ titer measurement y_{ijk} given values of the parameters.

Because our titer data are estimated and recorded in increments of $1/n_{wells}$ $\log_{10}TCID_{50}/mL$, where n_{wells} is the number of wells used for endpoint titration, our $\log_{10}$ titer values are interval-censored – only known to within a range of width $1/n_{wells}$. In addition, there is a degree of measurement noise in the titration process itself.

To model this, we assume that in each experimental condition i, there is a true underlying $\log_{10}$ titer x_{ijk} that is measured with some amount of experimental noise or error ε_{ijk} and then observed as an interval-censored value $y_{ijk} \approx x_{ijk} + \varepsilon_{ijk}$. We model the measurement errors ε_{ijk} as Normally distributed with a standard deviation σ_i that is shared by all samples in the given experimental condition; this reflects the fact that some experimental setups may be more or less noisy than others.

$$\varepsilon_{ijk} \sim \text{Normal}(0, \sigma_i)$$

We model the probability of observing an interval-censored $\log_{10}$ titer value y_{ijk} given a true underlying $\log_{10}$ titer x_{ijk} and a measurement error standard deviation σ_i as:

$$P(y_{ijk} \mid x_{ijk}, \sigma_i) = \text{NormalCDF}(y_{ijk}, x_{ijk}, \sigma_i) - \text{NormalCDF}(y_{ijk} - 1/n_{wells}, x_{ijk}, \sigma_i)$$

This reflects the probability given a true value x_{ijk} plus the measurement error $x_{ijk} + \varepsilon_{ijk}$ falls between $y_{ijk} - 1/n_{wells}$ and y_{ijk}. Due to the $\log_{10}$ titer imputation technique used, a titer in that range is most likely to be rounded up and reported as y_{ijk}.

The detection limit of our experiment is 0.5 $\log_{10}$ $TCID_{50}$/mL. The probability of observing an undetectable measured $\log_{10}$ titer value y_{ijk} given a true $\log_{10}$ titer value x_{ijk} is given by:

$$P(y_{ijk} \leq 0.5 \mid x_{ijk}, \sigma_i) = \text{NormalCDF}(0.5, x_{ijk}, \sigma_i)$$

We then model each replicate j for experimental condition i as starting with some true initial $\log_{10}$ titer $x_{ij}(0) = x_{ij0}$. We assume that viruses in experimental condition i decay exponentially at a rate λ_i over time t. It follows that

$$x_{ij}(t) = x_{ij0} - \lambda_i t$$

where t_k is the k^{th} measured time-point.

Model prior distributions

We place a weakly informative Normal prior distribution on the initial $\log_{10}$ titers x_{ij0} to rule out implausibly large or small values (e.g. in this case undetectable $\log_{10}$ titers or $\log_{10}$ titers much higher than the deposited concentration), while allowing the data to determine estimates within plausible ranges:

$$x_{ij0} \sim \text{Normal}(4.5, 2.5)$$

We likewise placed a weakly informative Half-Normal prior on the exponential decay rates λ_i:

$$\lambda_i \sim \text{Half-Normal}(0.5, 4)$$

We placed a weakly informative Half-Normal prior on the standard deviations of the experimental error distributions σ_i:

$$\sigma_i \sim \text{Half-Normal}(0, 2)$$

Markov Chain Monte Carlo Methods

We drew posterior samples using Stan, which implements a No-U-Turn Sampler (a form of Markov Chain Monte Carlo). We ran four replicate chains from random initial conditions for 2000 iterations, with the first 1000 iterations as a warmup/adaptation period. We saved the final 1000 iterations from each chain, giving us a total of 4000 posterior samples. We assessed convergence by inspecting trace plots and examining $\hat{R}$ and effective sample size (n_{eff}) statistics ($\hat{R}$ for all parameters ≤ 1.003, n_{eff} for all parameters $\geq$28% of total samples).

Supplemental table and figures

Table 1. Posterior median estimates and 95% credible intervals (2.5%–97.5% quantile range) for half-lives of HCoV-19 and SARS-CoV-1 in aerosols and on various surfaces, as well as a median estimate and 95% credible interval for the difference between the two half-lives (HCoV-19 – SARS-CoV-1).

	HCoV-19 half-life (hrs)			**SARS-CoV-1** half-life (hrs)			**HCoV-19 – SARS-CoV-1** difference (hrs)		
Material	*median*	*2.5%*	*97.5%*	*median*	*2.5%*	*97.5%*	*median*	*2.5%*	*97.5%*
Aerosols	1.09	0.64	2.64	1.18	0.778	2.43	-0.0913	-1.35	1.39
Copper	0.774	0.427	1.19	1.5	0.929	2.66	-0.735	-1.91	-0.0339
Cardboard	3.46	2.34	5	0.587	0.317	1.21	2.85	1.58	4.41
Steel	5.63	4.59	6.86	4.16	3.3	5.22	1.46	0.00127	2.96
Plastic	6.81	5.62	8.17	7.55	6.29	9.04	-0.722	-2.64	1.16

Figures S1–S5 (below) show Bayesian fits to individual replicate virus decay data for each virus. Replicates are shown in panel columns, viruses in panel rows. Lines are 50 random draws per panel from the posterior

distribution of fitted lines, to show level of uncertainty. Time axis is shown out to the latest time taken to reach an undetectable titer in the considered experimental conditions.

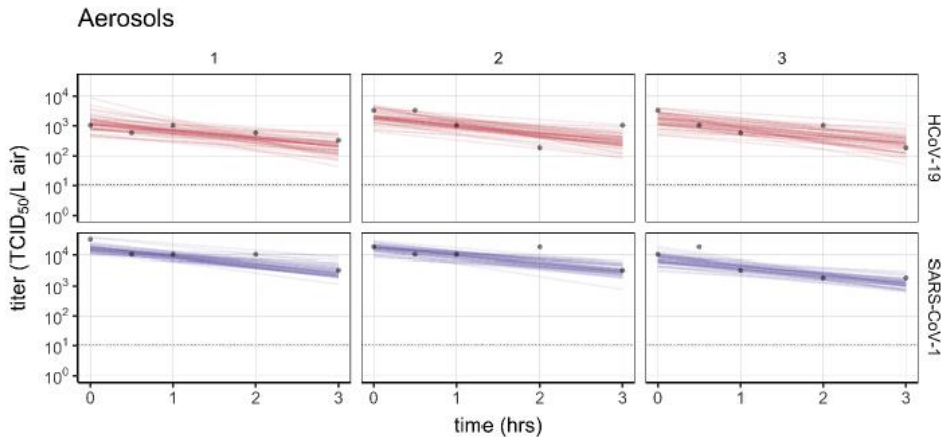

Figure S1. Individual replicate fits for aerosols. Columns show replicates, rows show virus (HCoV-19 above, SARS-CoV-1 below). Lines are 50 random draws per panel from the posterior distribution of fitted lines, to show level of uncertainty.

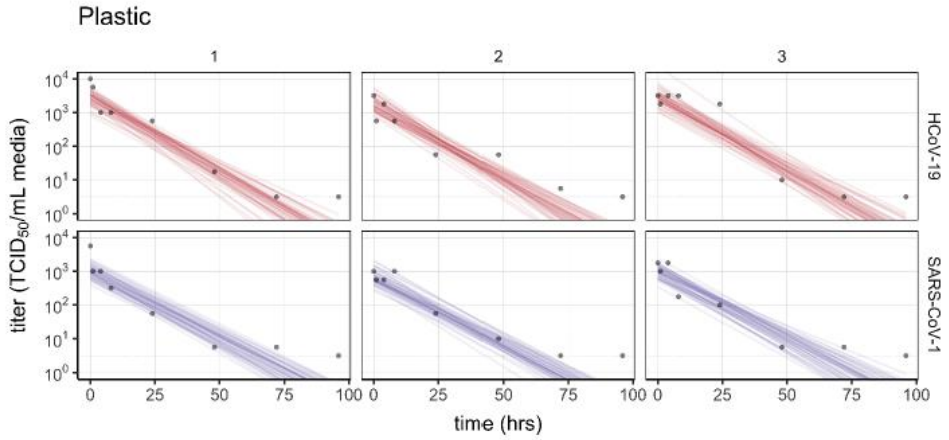

Figure S2. Individual replicate fits for plastic. Columns show replicates, rows show virus (HCoV-19 above, SARS-CoV-1 below). Lines are 50 random draws per panel from the posterior distribution of fitted lines, to show level of uncertainty.

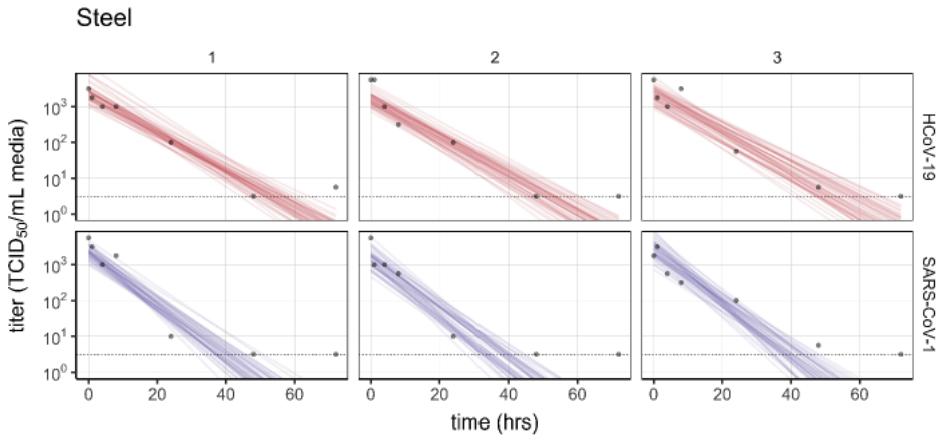

Figure S3. Individual replicate fits for steel. Columns show replicates, rows show virus (HCoV-19 above, SARS-CoV-1 below). Lines are 50 random draws per panel from the posterior distribution of fitted lines, to show level of uncertainty.

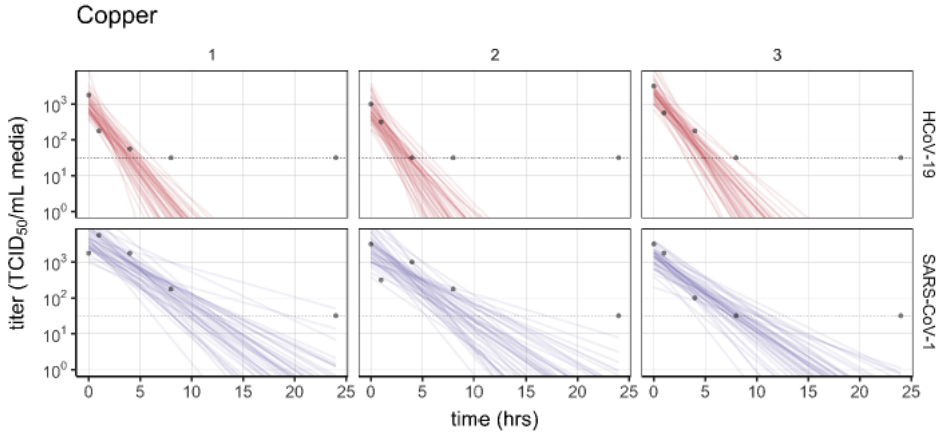

Figure S4. Individual replicate fits for copper. Columns show replicates, rows show virus (HCoV-19 above, SARS-CoV-1 below). Lines are 50 random draws per panel from the posterior distribution of fitted lines, to show level of uncertainty. Fits are substantially poorer for SARS-CoV-1 than for HCoV-19, and data do not follow a linear downward trend over time, suggesting that the difference in observed decay rates should be interpreted with caution.

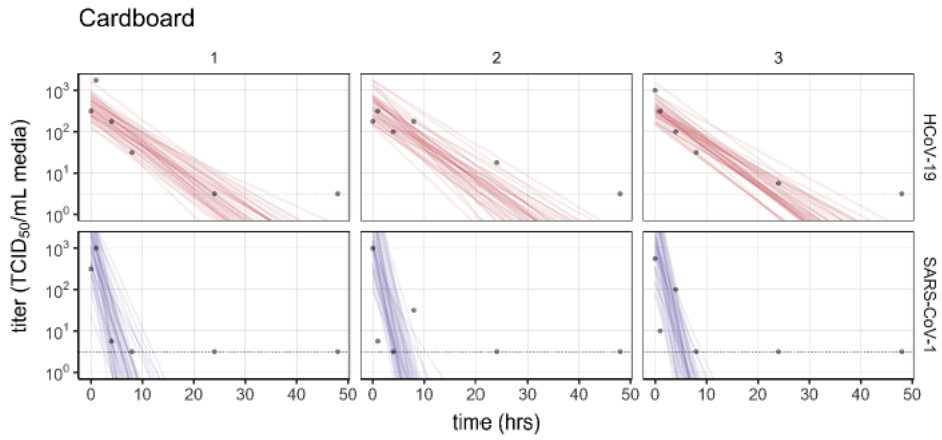

Figure S5. Individual replicate fits for cardboard. Columns show replicates, rows show virus (HCoV-19 above, SARS-CoV-1 below). Lines are 50 random draws per panel from the posterior distribution of fitted lines, to show level of uncertainty. Fits are substantially poorer for SARS-CoV-1 than for HCoV-19, and data do not follow a linear downward trend over time, suggesting that the difference in observed decay rates should be interpreted with caution.

Supplemental references

Fischer, R.J., Bushmaker, T., Judson, S., Munster, V.J., 2016. Comparison of the Aerosol Stability of 2 Strains of Zaire ebolavirus From the 1976 and 2013 Outbreaks. J. Infect. Dis. 214, 290–293.

Gelman, A., Carlin, J.B., Stern, H.S., Dunson, D.B., Vehtari, A., Rubin, D.B., 2013. Bayesian Data Analysis, Third Edition. CRC Press.

Holshue, M.L., DeBolt, C., Lindquist, S., Lofy, K.H., Wiesman, J., Bruce, H., Spitters, C., Ericson, K., Wilkerson, S., Tural, A., Diaz, G., Cohn, A., Fox, L., Patel, A., Gerber, S.I., Kim, L., Tong, S., Lu, X., Lindstrom, S., Pallansch, M.A., Weldon, W.C., Biggs, H.M., Uyeki, T.M., Pillai, S.K., 2020. First Case of 2019 Novel Coronavirus in the United States. N. Engl. J. Med. 382, 929–936.

Marra, M.A., Jones, S.J.M., Astell, C.R., Holt, R.A., Brooks-Wilson, A., Butterfield, Y.S.N., Khattra, J., Asano, J.K., Barber, S.A., Chan, S.Y., Cloutier, A., Coughlin, S.M., Freeman, D., Girn, N., Griffith, O.L., Leach, S.R., Mayo, M., McDonald, H., Montgomery, S.B., Pandoh, P.K., Petrescu, A.S., Robertson, A.G., Schein, J.E., Siddiqui, A., Smailus, D.E., Stott, J.M., Yang, G.S., Plummer, F., Andonov, A., Artsob, H., Bastien, N., Bernard, K., Booth, T.F., Bowness, D., Czub, M., Drebot, M., Fernando, L., Flick, R., Garbutt, M., Gray, M., Grolla, A., Jones, S., Feldmann, H., Meyers, A.,

149 Kabani, A., Li, Y., Normand, S., Stroher, U., Tipples, G.A., Tyler, S., Vogrig, R., Ward, D., Watson,
150 B., Brunham, R.C., Krajden, M., Petric, M., Skowronski, D.M., Upton, C., Roper, R.L., 2003. The
151 Genome sequence of the SARS-associated coronavirus. Science 300, 1399–1404.
152 van Doremalen, N., Bushmaker, T., Munster, V., 2013. Stability of Middle East respiratory syndrome
153 coronavirus (MERS-CoV) under different environmental conditions. Eurosurveillance 18, 20590.
154 Zou, L., Ruan, F., Huang, M., Liang, L., Huang, H., Hong, Z., Yu, J., Kang, M., Song, Y., Xia, J., Guo,
155 Q., Song, T., He, J., Yen, H.-L., Peiris, M., Wu, J., 2020. SARS-CoV-2 Viral Load in Upper
156 Respiratory Specimens of Infected Patients. N. Engl. J. Med. In press.

157 **Code and data availability**

158 Code and data to reproduce the Bayesian estimation results and produce corresponding figures are
159 archived online at OSF: https://doi.org/10.17605/OSF.IO/FB5TW and available on Github:
160 https://github.com/dylanhmorris/sars-cov-2-stability

161 **Acknowledgements**

162 We would like to thank Kwe Claude Yinde and Michael Letko for experimental assistance. This
163 research was supported by the Intramural Research Program of the National Institute of Allergy and
164 Infectious Diseases (NIAID), National Institutes of Health (NIH). JOL-S and AG were supported by the
165 Defense Advanced Research Projects Agency DARPA PREEMPT # D18AC00031, and JOL-S was
166 supported by the U.S. National Science Foundation (DEB-1557022) and the Strategic Environmental
167 Research and Development Program (SERDP, RC-2635) of the U.S. Department of Defense. The findings
168 and conclusions in this report are those of the author(s) and do not necessarily represent the official position
169 of the Centers for Disease Control and Prevention. Names of specific vendors, manufacturers, or products
170 are included for public health and informational purposes; inclusion does not imply endorsement of the
171 vendors, manufacturers, or products by the Centers for Disease Control and Prevention or the US
172 Department of Health and Human Services.

CHAPTER THREE

COMPARATIVE AEROSOL STABILITY OF SARS-CoV-2 VARIANTS OF CONCERN

Contribution of Authors and Co-Authors

Manuscript in Chapter 3

Author: Trenton Bushmaker

Contributions: Conceptualization, writing, methodology, data curation, and visualization.

Author: Claude Kwe Yinda

Contributions: Conceptualization, writing, methodology, data curation, and visualization.

Author: Dylan H. Morris

Contributions: Conceptualization, data curation, visualization, and writing.

Co-Author: Myndi G. Holbrook

Contributions: Methodology.

Co-Author: Amandine Gamble

Contributions: Data curation and visualization.

Co-Author: Danielle Adney

Contributions: Methodology.

Co-Author: Cara Bushmaker

Contributions: Resources.

Co-Author: Neeltje van Doremalen

Contributions: Resources and visualization

Co-Author: Raina K. Plowright

Contributions: Supervision and writing.

Co-Author: James O. Lloyd-Smith

Contributions: Conceptualization, writing, and supervision.

Co-Author: Vincent J. Munster

Contributions: Conceptualization, writing, supervision and resources.

Manuscript Information

Trenton Bushmaker, Claude Kwe Yinda, Dylan H. Morris, Myndi G. Holbrook, Amandine Gamble, Danielle Adney, Cara Bushmaker, Neeltje van Doremalen, Raina K. Plowright, James O. Lloyd-Smith, and Vincent J. Munster

Target submission journal - Emerging Infectious Diseases – CDC

Status of Manuscript:
_X_ Prepared for submission to a peer-reviewed journal
____ Officially submitted to a peer-reviewed journal
____ Accepted by a peer-reviewed journal
___ Published in a peer-reviewed journal

Comparative aerosol stability of SARS-CoV-2 Variants of Concern

Trenton Bushmaker[1,2*], Claude Kwe Yinda[1*], Dylan H. Morris[3*], Myndi G. Holbrook[1], Amandine Gamble[3], Danielle Adney[1#], Cara Bushmaker[5], Neeltje van Doremalen[1], Raina K. Plowright[2], James O. Lloyd-Smith[3,4], Vincent J. Munster[1]

1. Laboratory of Virology, Division of Intramural Research, National Institute of Allergy and Infectious Diseases, National Institutes of Health, Hamilton, MT, USA
2. Dept. of Microbiology and Cell Biology, Montana State University, Bozeman, MT, USA
3. Dept. of Ecology and Evolutionary Biology, University of California, Los Angeles, Los Angeles, CA, USA
4. Fogarty International Center, National Institutes of Health, Bethesda, MD, USA
5. Bitterroot Health - Daly Hospital, Hamilton, MT, USA

* These authors contributed equally to this article

Current affiliation: Lovelace Biomedical Research Institute, Dept. of Comparative Medicine, Albuquerque, NM, USA

Introduction

In December 2019, SARS-CoV-2 first emerged in Wuhan, China. Epidemiological studies suggest that airborne transmission is one of the major routes of human-to-human transmission [28]. Infectious SARS-CoV-2 has been detected in exhaled aerosols from hospitalized patients and mild human cases [3, 29, 30]. Experimentally airborne and fine aerosol transmission (aerosols <5 µm) has been shown for SARS-CoV-2 in hamster and ferret animal models [1, 18, 31-33]. Human-to-human transmission can be compartmentalized into shedding from an infected person, environmental stability, and onward transmission, and finally the susceptibility of the exposed person [34]. In the early phase of the SARS-CoV-2 epidemic we investigated the stability of the virus on surfaces and in aerosols. Linked with the epidemiological data at that time, the aerosol stability of SARS-CoV-2 indicated that aerosol transmission of SARS-CoV-2 was plausible, since the virus can remain viable and infectious in aerosols for hours [23]. The aerosol stability of SARS-CoV-2 has now been confirmed by several research groups [35, 36].

Since the initial emergence of SARS-CoV-2 (Lineage A), new lineages and variants have emerged typically replacing previously circulating lineages [37]. Within these novel emerging SARS-CoV-2 lineages, variants of concern (VOCs) are of particular interest. VOCs are defined by phenotypic changes including enhanced transmission, increased pathogenicity, and decreased efficacy of prophylactic and therapeutic countermeasures. As of November 26, 2021, five variants had been characterized as Variants of Concern (VOCs) by the World Health Organization [38]. The evolutionary mechanism behind the emergence of VOCs is still poorly understood, although enhanced transmission and immune evasion have been proposed as most

likely mechanisms [39]. To assess whether the ongoing evolution of SARS-CoV-2 resulted in changes in the aerosol stability between different strains, we directly compared the original Lineage A ancestral virus with viruses and VOCs from later timepoints during the pandemic.

Materials and Methods

Cells and viruses

SARS-CoV-2 strains were passaged once on VeroE6 cells maintained in DMEM supplemented with 10% FBS, 2 mM L-glutamine, 100 U/ml penicillin and 100 µg/ml streptomycin.

The ancestral WA1 (lineage A) strain hu/USA/CA_CDC_5574/2020 (MN985325.1) was provided by CDC, Atlanta, USA. The B.1 hCoV-19/USA/MT-RML-7/2020 (GISAID# EPI_ISL_591054, MW127503.1) was derived from a clinical specimen obtained from Bitterroot Health - Daly Hospital Hamilton, USA. For the VOCs, Alpha variant B.1.1.7 hCOV_19/England/204820464/2020, NR-54000 (GISAID#EPI_ISL_683466) was obtained through BEI Resources, NIAID, NIH: Severe Acute Respiratory Syndrome-Related Coronavirus 2, contributed by Dr. Bassam Hallis. Beta variant B.1.351 hCoV-19/USA/MD-HP01542/2021 (GISAID# EPI_ISL_890360) was acquired from Dr. Tulio de Oliveira and Dr. Alex Sigal at the Nelson R. Mandela School of Medicine, UKZN. The Delta variant B.1.617.2 hCoV-19/USA/KY-CDC-2-4242084/2021 (GISAID# EPI_ISL_1823618) was obtained from BEI and the Omicron variant B.1.1.529 hCoV-19/USA/WI-WSLH-221686/2021 ((GISAID# EPI_ISL_7263803 was obtained from Drs. Peter Halfmann and Yoshihiro Kawaoka at the University of Wisconsin – Madison, USA (Table 1).

All virus stocks were propagated in VeroE6 cells in DMEM supplemented with 2% fetal bovine serum (FBS), 2 mM L-glutamine, 100 U/ml penicillin and 100 µg/ml streptomycin. Stocks were harvested between Day 4 - 6, dependent of the cytopathic effect. Supernatant was collected to be centrifuged at 1200 rpm for 8 minutes at room temperature centrifugation and frozen at −80°C. No variations or containments were detected, via deep sequencing with the Illumina MiSeq system using nano 300-cycle chemistry (Illumina); isolates used for aerosol generation were identical to the initial deposited GenBank or GISAID sequences.

Goldberg drum exposure and sample analysis

Droplet nuclei size particles (<5 µm) were generated using a 3-jet Collison nebulizer (CH Technologies) containing $10^{5.75}$ - 10^{6} $TCID_{50}$/mL in 10 mL of DMEM supplemented with 2% FBS. The inoculum fed into a rotating Goldberg drum (Biaera Technologies) to create an aerosolized environment. The drum system was prepared until a starting environment of 65% relative humidity (RH) and a temperature of 21-23°C was reached for all SARS-CoV-2 Goldberg drum runs. Aerosols were maintained in suspension with a rotation of 3 mph to overcome terminal settling velocity.

Three independent replicates were performed for each of the respective timepoint, either a 3 hour or 8 hour run for each of the SARS-CoV-2 strains assessed in this study. For each independent run, samples were collected at 0 and 3-hour or 0 and 8-hour post aerosol generation. Samples were collected by drawing air at 6 LPM for 30 secs onto a 47mm gelatin filter (Sartorius). Filters were dissolved in 10 mL of DMEM containing 10% FBS at 37°C. Samples were frozen at -80°C until assessment.

Aerosol sample quantification

Aerosol samples were quantified using qRT-PCR as previously described [40]. In short, 140 µL of sample was utilized for RNA extraction using the QIAamp Viral RNA Kit (Qiagen) using QIAcube HT automated system (Qiagen) with an elution volume of 150 µL. SARS-CoV-2 was detected using the E gene assay in a qRT-PCR (Corman et al., 2020) using 5 ul of input RNA and the TaqMan™ Fast Virus One-Step Master Mix (Applied Biosystems) and run on a QuantStudio 6 Flex Real-Time PCR System (Applied Biosystems). 10-fold dilutions SARS-CoV-2 E gene run-off transcripts 10-fold dilutions with known genome copies were run in parallel to allow calculation of genome copies in samples.

Infectious virus titers were determined by end-point titration on VeroE6 cells and TCID50/mL was calculated using method of Spearman-Karber on VeroE6 cells.

Spike Entry assay

Plasmids

The spike coding sequences for SARS-CoV-2 WA1, B.1, Alpha, Beta, Delta, and Omicron were designed using a truncated by deleting 19 amino acids at the C terminus. These sequences were codon optimized for human cells then appended with a 5′ kozak expression sequence (GCCACC) and 3′ tetra-glycine linker followed by nucleotides encoding a FLAG-tag sequence (DYKDDDDK). These spike sequences were synthesized and cloned into pcDNA3.1^{+}(GenScript). All DNA constructs were verified by Sanger sequencing (ACGT).

Pseudotype production and Luciferase-based cell entry assay

Pseudotype production and the entry assay was carried out as described previously [41]. Briefly, plates pre-coated with poly-L-lysine (Sigma–Aldrich) were seeded with 293T cells and transfected the following day with 1,200 ng of empty plasmid and 400 ng of plasmid encoding coronavirus spike or no-spike plasmid control (green fluorescent protein (GFP)). After 24 h, transfected cells were infected with VSVΔG seed particles pseudotyped with VSV-G. After one hour of incubation with intermittent shaking at 37 °C, cells were washed four times and incubated in 2 mL DMEM supplemented with 2% FBS, penicillin/streptomycin and L-glutamine for 48 h. Supernatants were collected, centrifuged at 500xg for 5 min, aliquoted and stored at −80 °C. VeroE6 cells were inoculated with equivalent volumes of pseudotype stocks. Plates were then centrifuged at 1200xg at 4 °C for one hour and incubated overnight at 37 °C. Approximately 18–20 h post-infection, Bright-Glo luciferase reagent (Promega) was added to each well, 1:1, and luciferase was measured. The relative entry was calculated by normalizing the relative light unit for spike pseudotypes to the to the no-spike control.

Results

For these experiments, we selected the following SARS-CoV-2 strains to represent the following lineages using PANGO nomenclature: Lineage A, strain hu/USA/CA_CDC_5574/2020 (WA1) representing the ancestral lineage of SARS-CoV-2 [42] , Lineage B1, hCoV-19/USA/MT-RML-7/2020 (B1) emerged in early 2020 largely defined by the D614G amino acid substitution in the S1 region of the spike glycoprotein (S) [43], Lineage B.1.1.7, hCOV_19/England/204820464/2020 (Alpha) emerged in November 2020 and defined by several S1 and S2 deletions and amino acid substitutions notably N501Y involved in

increased cellular entry [44]. Lineage B.1.351, hCoV-19/USA/MD-HP01542/2021 (Beta) emerged in December 2020 and is defined by a E to K substitution at position 484, involved in a moderate change in antigenicity [45], Lineage B.1.617.2, hCoV-19/USA/KY-CDC-2-4242084/2021 (Delta) which emerged in October 2020 which exhibited several amino acid substitutions and deletions, most notably the P to R substitution at position 681 involved in increased S cleavage efficiency [46, 47] and lastly the Lineage B.1.1.529 hCoV-19/USA/WI-WSLH-221686/2021 (Omicron), displaying the most amino acid substitutions of any variant detected to present, in particular in the receptor binding domain (RBD) of the S glycoprotein. The change in RBD has resulted in a dramatic change in antigenicity and subsequent humoral immune escape [48] (Table 1.).

To assess the impact of these changes in S between the different variants, we evaluated the infectivity of above listed variants in vitro with the S glycoprotein of each of these lineages pseudotyped on vesicular stomatitis virus (VSV) particle. The relative entry of the pseudo virus particles of all the variants was compared to the entry of the original ancestral strains WA1. Starting with the B1, a roughly 2.97-fold increase in relative entry efficiency was observed over the WA1 ancestral lineage. This increase in relative entry efficiency remained conserved over the duration of the emergence of Alpha, Beta, and Delta. However, the VSV-particles pseudotyped with the S of the Omicron variant had a relative entry efficiency similar to that of WA1 (Figure 1D). This suggest that the mutations observed in the S of Omicron resulted in significant antigenic escape from preexisting immunity but at the loss of some of the increase in relative entry efficiency observed in the lineages B1 to Delta.

Next, we assessed whether the continuous evolution of SARS-CoV-2 and the associated amino acid substitutions and deletions had an impact on the previously reported aerosol stability [23, 35, 36, 49]. We directly compared the exponential decay of different SARS-CoV-2 isolates using 0, 3 and 8 hours as our time points. These experiments were either run as a single 0 to 3 hours run or a 0 to 8 hours run, with sample collection at the start point and the end point. For all SARS-CoV-2 strains used, the runs were conducted in triplicate. To determine the exponential decay in the samples over time, the air samples collected at 0, 3 or 8 hours post aerosolization were analyzed by quantitative real-time polymerase chain reaction (qRT-PCR) for the SARS-CoV-2 E-gene to determine the amount of genome copies within the samples. To determine the actual amounts of viable SARS-CoV-2, the samples were titrated on Vero E6 cells to determine the concentration of infectious virus within the samples. Using the calculated genome copies, the samples were normalized, and the decay was calculated relative to the amount of genome copies.

All the analyzed SARS-CoV-2 isolates remained viable in aerosols throughout the 8-hour duration of our experiment (Figure 1A) and all viruses had an exponential decay in virus titer across all experimental conditions, as indicated by a linear decrease in the log10$TCID_{50}$ per liter of air or milliliter of medium over time (Figure 1B). The posterior median [95% credible interval] half-life of SARS-CoV-2 the ancestral lineage WA1 was 2.85 [2.04, 4.49]. The B.1, Alpha and Beta viruses appeared to have longer half-lives than WA1: 3.83 [2.52, 8] for B.1, 4.62 [2.6, 14.4] for Alpha, and 4.78 [2.86, 13.8] for Beta. The Delta variant displayed a half-life similar to that of WA1: 2.82 [2.01, 4.62]. The Omicron variant displayed a similar or slightly decreased half-life compared to WA1: 1.92 [1.23, 3.54] (Figure 1B). We estimated half-life changes relative to WA1 by calculating the posterior median fold-change in half-life compared

to WA1. Estimated fold-changed were 1.36 [0.706, 2.85] for B.1, 1.57 [0.767, 3.68] for Alpha, 1.85 [0.738, 4.95] for Beta, 1.07 [0.443, 2.64] for Delta, and 0.808 [0.411, 1.87] for Omicron.

When analyzing the relative half-life fold change over WA1, we see an initial moderate increase in stability with B1, Alpha and Beta, followed by similar relative half-live for Delta and a slightly decreased half-life for Omicron (Figure 1C). Interestingly, the increase in amino acid substitutions over WA1 resulted in an initial increase in relative stability. However, additional amino acid substitutions resulted in a decrease in stability comparable to the level of WA1 that was further exacerbated with Omicron (Figure 2).

Discussion

We are currently in the third year since the emergence of SARS-CoV-2 in China, 2019. As of March 11 2022, SARS-CoV-2 has infected an estimated 452 million people, causing more than 6 million deaths [50]. Continuous circulation of SARS-CoV-2 in the human population has seen the generation and turnover of multiple distinct SARS-CoV-2 lineages [51]. With the increase in full genome sequencing, changes within the genome and changes in relative frequency of lineages are tracked in real-time [52].

The ongoing evolution of SARS-CoV-2 has resulted in lineages under specific scrutiny such as the Variants of Concern (VoC). A variant is termed a VoC if it is associated with an increase in transmission or virulence, or a decrease in the effectiveness of public health and social measures, such as diagnostics, vaccines, or therapeutics [53]. Data on the phenotypic characteristics of these VoCs are typically focused on vaccine and mAb efficacy and diagnostic assay performance [54].

One of the hallmarks of some of the VoCs, such as Alpha, Delta and Omicron is the rapid replacement of the previously dominant variant by a new one (reviewed in reference [55]). Currently the Omicron BA.2 subvariant appears to be replacing the Omicron BA.1 VoC. Mechanistically, the replacement of existing variant by new ones has been thought to be caused by intrinsic increase in the transmission phenotype [56], escape from preexisting immunity, or a combination of both [56, 57].

One of the major routes of transmission of SARS-CoV-2 is via the aerosol route. Mechanistically the aerosol route can be delineated by the factors affecting the donor host (e.g., peak shedding, duration of shedding and aerosol generation), the environmental (e.g., aerosol stability, dilution, airflow), and the recipient host (e.g., infectious dose, route of exposure, and intrinsic susceptibility and immune status) [3, 34, 58].

To understand the relationship between the ongoing SARS-CoV-2 evolution, in the context of the accumulation of mutations predominantly in the S glycoprotein, we analyzed phenotypic characteristics of a wide set of SARS-CoV-2 viruses. One of the key phenotypic changes associated with emergence of novel variants is an increase in ability to effectively bind to the receptor ACE2. Several reports have consistently shown an increase of the binding potential starting with the D614G of B.1 D614G, B.1.1.7, and B.1.351 [59-61], suggesting that one of the major evolutionary selective pressures was an increase in the efficiency of binding to the angiotensin converting enzyme 2 (ACE2), which likely has a direct effect on transmission by lowering the infectious dose needed for infection. Computational studies indicate an increase in binding efficiency for Omicron over Delta [62], whereas in vitro SPR analyses show a similar binding profile between Delta and Omicron. Interestingly, using a pseudotype VSV-assay, which

assess the actual entry of particles in cells, the increase in entry efficiency of the D614G, Alpha, Beta and Delta was confirmed. However, the Omicron VoC displays entry kinetics similar to that of the ancestral strain WA1, suggesting that the multitude of mutations allowing antigenic escape reduced the entry potential of this VoC slightly. This less fusogenic spike, via a neutralization protected closed RBD, with increased transmission could be explained by its resistance to misfiring before reaching a new host during respiratory transmission [39].

Several studies have analyzed the stability of SARS-CoV-2 in aerosols in a Goldberg rotating drum set-up. In general, these studies focused on the duration of the detection of infectious viruses, which in some studies was detected even after 16 hours [35] and the calculation of the respective half-lives of the virus within the aerosol. Studies using the VoCs B.1 and B.1.1.7 did not observe any notable differences in aerosol stability between the original (WA1) hCoV-19/USA/WA-1/2020 (NR-52281) strain and the VoCs (B.1) hCoV-19/USA/NY-PV08449 (NR-53515) and (B.1.1.7) hCoV-19/USA/CA_CDC_5574/2020 [36].

Within our study, we have modified the experimental setup of our initial experiment's with WA1 to independent runs of either three or eight hours to be better able to capture subtle changes in aerosol stability. Within our studies we see in initial increase in aerosol stability with the D614G, Alpha and Beta variants over the ancestral WA1, followed by a drop to a similar half-live as WA1 for Delta and a slight decrease in half-life for Omicron.

Our study suggests that aerosol stability per se is likely not a major factor in the increase in transmission or the replacement of previously circulation lineages by new ones. Epidemiological and experimental studies suggest that the window for transmission is typically relative short (under an hour), and that a relatively modest decrease in half-life will not have any impact on the

population epidemiological level [63]. However, at the individual level it will remain important to understand the relative window for transmission after the release of SARS-CoV-2 containing aerosols from an infected individual.

Interestingly, the emergence of Omicron coincides with a dramatic change in the immune landscape, where people have either been vaccinated or previously exposed to SARS-CoV-2. The amino acid changes in the S glycoprotein result in a dramatic antigenic change and drops in neutralizing titers of over 40-fold have been reported with human sera from either previously exposed or vaccinated individuals [64]. This suggests that in contrast to the previous lineages where the major evolutionary pressure was directed at an increase in transmission, it is currently directed it towards antigenic escape.

Acknowledgements

We would like to thank Michele Adams for clinical specimen acquisition, Ricki Feldmann for experimental support and RML Genomics Unit's Dr. Craig Martens and Stacey Ricklefs for sequencing expertise. This research was supported by the Intramural Research Program of the National Institute of Allergy and Infectious Diseases (NIAID), National Institutes of Health (NIH) and Defense Advanced Research Projects Agency DARPA PREEMPT # D18AC00031. The content of the article does not necessarily reflect the position or the policy of the U.S. government, and no official endorsement should be inferred.

Author contributions

Conceptualization: T.B., C.K.Y., A.G., D.M., V.M., and J.L.S; methodology: T.B., C.K.Y., M.H., and D.R.A.; resources: C.I.B. and N.v.D.; supervision: V.J.M. and R.K.P.; data curation: T.B., C.K.Y and D.M..; writing: T.B., C.K.Y., A.G., D.M., R.K.P., V.M., and J.L-S.; visualization: T.B., C.K.Y., A.G., and D.M.

Isolate	WHO Labe	PANGO	GISAID/GenBank	18	19	67	69	70	80	95	142	143	144	145	156	157	158	211	212	214	215	241	242	243	339	371	373	375	417	440	446	452	477	478	484	493	496	498	501	505	547	570	614	655	679	681	701	716	764	796	856	950	954	969	981	982	1118
hu/USA/CA_CDC_5574/2020	-	A	MN985325.1	L	T	A	H	V	D	T	G	V	Y	Y	E	F	R	N	L	R	D	L	L	A	G	S	S	S	K	N	G	L	S	T	E	Q	G	Q	N	Y	T	A	D	H	N	P	A	T	N	D	N	D	Q	N	L	S	D
hCoV-19/USA/MT-RML-7/2020	-	B.1	EPI_ISL_591054/MW127503	L	T	A	H	V	D	T	G	V	Y	Y	E	F	R	N	L	R	D	L	L	A	G	S	S	S	K	N	G	L	S	T	E	Q	G	Q	N	Y	T	A	G	H	N	P	A	T	N	D	N	D	Q	N	L	S	D
hCoV-19/England/204820464/2020	Alpha	B.1.1.7	EPI_ISL_683466	L	T	A	DEL	DEL	D	T	G	V	DEL	Y	E	F	R	N	L	R	D	L	L	A	G	S	S	S	K	N	G	L	S	T	E	Q	G	Q	Y	Y	T	D	G	H	N	H	A	I	N	D	N	D	Q	N	L	A	H
hCoV-19/USA/MD-HP01542/2021	Beta	B.1.351	EPI_ISL_890360	F	T	A	H	V	A	T	G	V	Y	Y	E	F	R	N	L	R	G	DEL	DEL	DEL	G	S	S	S	N	N	G	L	S	T	K	Q	G	Q	Y	Y	T	A	G	H	N	P	V	T	N	D	N	D	Q	N	L	S	D
hCoV-19/USA/KY-CDC-2-4242084/20	Delta	B.1.617.2	EPI_ISL_1823618	L	R	A	H	V	D	T	D	V	Y	Y	DEL	DEL	G	N	L	R	D	L	L	A	G	S	S	S	K	N	G	R	S	K	E	Q	G	Q	N	Y	T	A	G	H	N	R	A	T	N	D	N	N	Q	N	L	S	D
hCoV-19/USA/WI-WSLH-221686/202	Omicron	B.1.1.529	EPI_ISL_7263803	L	T	V	DEL	DEL	D	I	D	DEL	DEL	DEL	E	F	R	DEL	I	REPE	D	L	L	A	D	L	P	F	N	K	S	L	N	K	A	R	S	R	Y	H	K	A	G	Y	K	H	A	T	K	Y	K	D	H	K	F	S	D
				S1																																																				S2								
																									RBD																																					

Table 1. SARS-CoV-2 Isolates and mutations

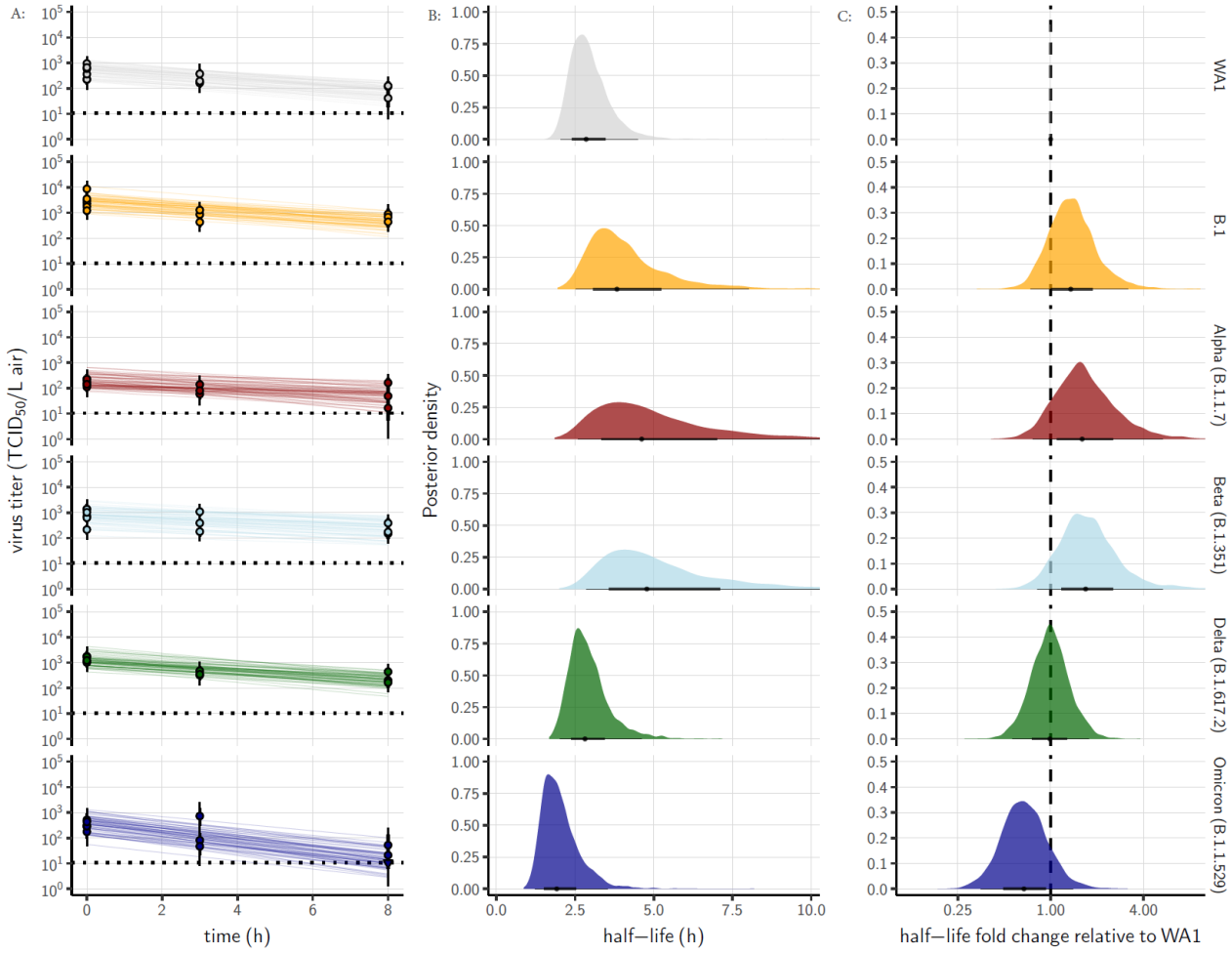

Figure 1. Exponential decay rates and corresponding half-lives for SARS-CoV-2 for ancestral cohort and Variants of Concern (VOCs). A: Regression plots showing predicted decay of log10 virus titer over time normalized by qRT-PCR. Points show measured titers. Lines are random draws from the joint posterior distribution of the exponential decay rate (negative of the slope) and intercept (initial virus titer); thus visualizing the range of possible decay patterns for each experimental condition. 150 lines per panel: 50 lines from each plotted replicate. B: Plots showing posterior distribution of viable virus. Dot shows the posterior median estimate and black line shows a 95% credible interval. C: Plots showing posterior distribution for half-life fold change of viable virus compared to the WA1 strain. Dot shows the posterior median estimate and black line shows a 95% credible interval. D: Plot shows the relative entry of the pseudotype particles of each virus in relationship to no-entry control (GFP).

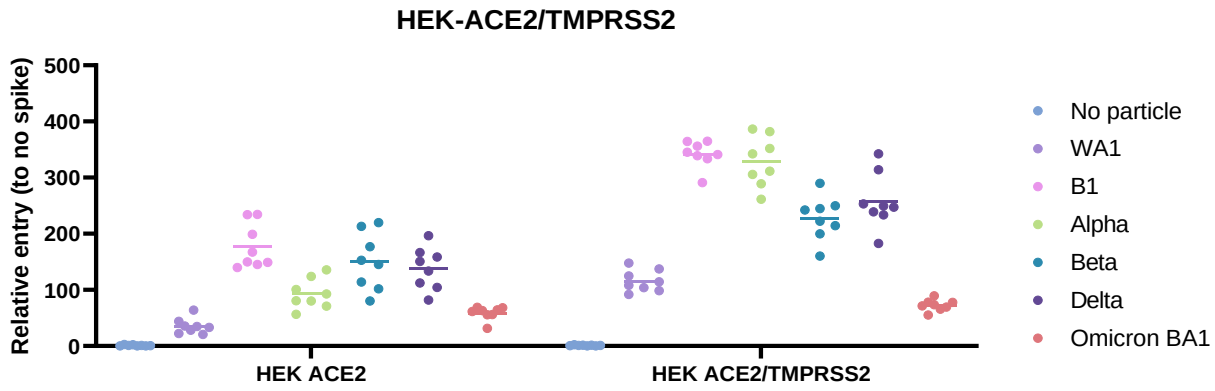

Figure 1D: Virus Entry data

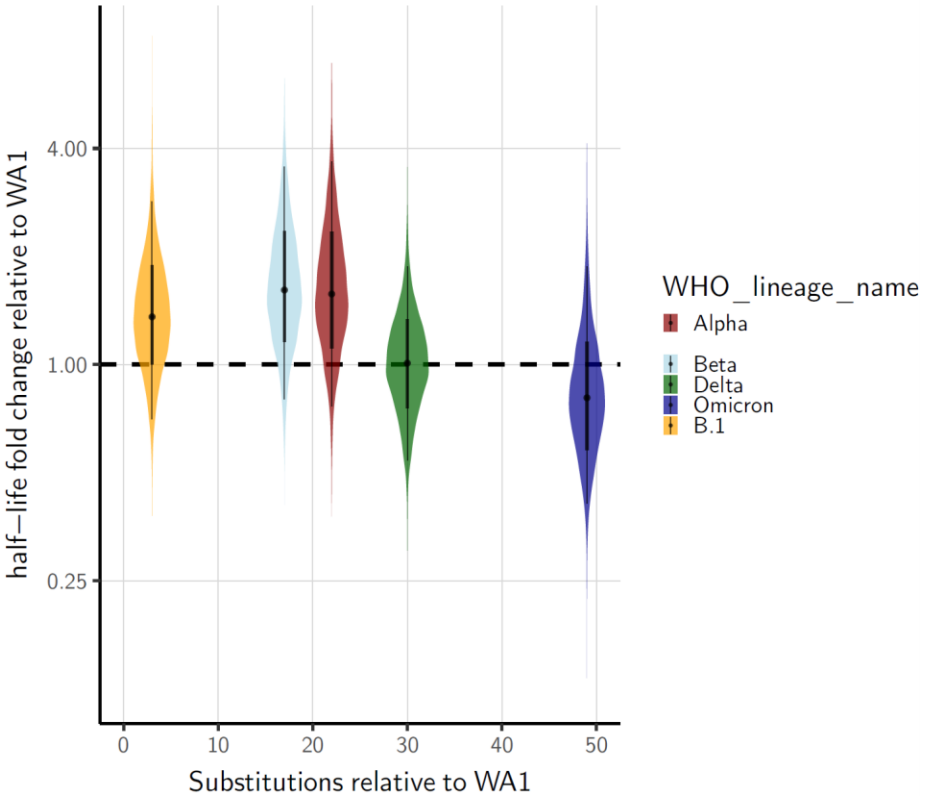

Figure 2. Correlation of the half-lives of the ancestral cohort or Variants of Concern in proportion of the substitution ammino acid changes to the complete viral genome SARS-CoV-2 relative to the WA1 Lineage A.

Manuscript References:

Adenaiye, O. O., Lai, J., de Mesquita, P. J. B., Hong, F., Youssefi, S., German, J., Tai, S. S., Albert, B., Schanz, M., Weston, S., Hang, J., Fung, C., Chung, H. K., Coleman, K. K., Sapoval, N., Treangen, T., Berry, I. M., Mullins, K., Frieman, M., Ma, T., Milton, D. K., & University of Maryland Stop, C. R. G. (2021). Infectious SARS-CoV-2 in Exhaled Aerosols and Efficacy of Masks During Early Mild Infection. *Clin Infect Dis*. https://doi.org/10.1093/cid/ciab797

Andrew Rambaut, N. L., Oliver Pybus, Wendy Barclay, Jeff Barrett, Alesandro Carabelli, Tom Connor, Tom Peacock, David L Robertson, Erik Volz, on behalf of COVID-19 Genomics Consortium UK (CoG-UK). (2020). Preliminary genomic characterisation of an emergent SARS-CoV-2 lineage in the UK defined by a novel set of spike mutations. *Virological*, *Dec. 2020*. https://virological.org/t/563

Chen, J., & Wei, G. W. (2022). Omicron BA.2 (B.1.1.529.2): high potential to becoming the next dominating variant. *Res Sq*. https://doi.org/10.21203/rs.3.rs-1362445/v1

Coleman, K. K., Tay, D. J. W., Sen Tan, K., Ong, S. W. X., Son, T. T., Koh, M. H., Chin, Y. Q., Nasir, H., Mak, T. M., Chu, J. J. H., Milton, D. K., Chow, V. T. K., Tambyah, P. A., Chen, M., & Wai, T. K. (2021). Viral Load of SARS-CoV-2 in Respiratory Aerosols Emitted by COVID-19 Patients while Breathing, Talking, and Singing. *Clin Infect Dis*. https://doi.org/10.1093/cid/ciab691

Corman, V. M., Landt, O., Kaiser, M., Molenkamp, R., Meijer, A., Chu, D. K., Bleicker, T., Brunink, S., Schneider, J., Schmidt, M. L., Mulders, D. G., Haagmans, B. L., van der Veer, B., van den Brink, S., Wijsman, L., Goderski, G., Romette, J. L., Ellis, J., Zambon, M., Peiris, M., Goossens, H., Reusken, C., Koopmans, M. P., & Drosten, C. (2020). Detection of 2019 novel coronavirus (2019-nCoV) by real-time RT-PCR. *Euro Surveill*, *25*(3). https://doi.org/10.2807/1560-7917.ES.2020.25.3.2000045

Dhar, M. S., Marwal, R., Vs, R., Ponnusamy, K., Jolly, B., Bhoyar, R. C., Sardana, V., Naushin, S., Rophina, M., Mellan, T. A., Mishra, S., Whittaker, C., Fatihi, S., Datta, M., Singh, P., Sharma, U., Ujjainiya, R., Bhatheja, N., Divakar, M. K., Singh, M. K., Imran, M., Senthivel, V., Maurya, R., Jha, N., Mehta, P., A, V., Sharma, P., Vr, A., Chaudhary, U., Soni, N., Thukral, L., Flaxman, S., Bhatt, S., Pandey, R., Dash, D., Faruq, M., Lall, H., Gogia, H., Madan, P., Kulkarni, S., Chauhan, H., Sengupta, S., Kabra, S., Indian, S.-C.-G. C. d. d., Gupta, R. K., Singh, S. K., Agrawal, A., Rakshit, P., Nandicoori, V., Tallapaka, K. B., Sowpati, D. T., Thangaraj, K., Bashyam, M. D., Dalal, A., Sivasubbu, S., Scaria, V., Parida, A., Raghav, S. K., Prasad, P., Sarin, A., Mayor, S., Ramakrishnan, U., Palakodeti, D., Seshasayee, A. S. N., Bhat, M., Shouche, Y., Pillai, A., Dikid, T., Das, S., Maitra, A., Chinnaswamy, S., Biswas, N. K., Desai, A. S., Pattabiraman, C., Manjunatha, M. V., Mani, R. S., Arunachal Udupi, G., Abraham, P., Atul, P. V., & Cherian, S. S. (2021). Genomic characterization and epidemiology of an emerging SARS-CoV-2 variant in Delhi, India. *Science*, *374*(6570), 995-999. https://doi.org/10.1126/science.abj9932

Fears, A. C., Klimstra, W. B., Duprex, P., Hartman, A., Weaver, S. C., Plante, K. S., Mirchandani, D., Plante, J. A., Aguilar, P. V., Fernandez, D., Nalca, A., Totura, A., Dyer, D., Kearney, B., Lackemeyer, M., Bohannon, J. K., Johnson, R., Garry, R. F., Reed, D.

S., & Roy, C. J. (2020). Persistence of Severe Acute Respiratory Syndrome Coronavirus 2 in Aerosol Suspensions. *Emerg Infect Dis*, *26*(9). https://doi.org/10.3201/eid2609.201806

Grabowski, F., Kochanczyk, M., & Lipniacki, T. (2022). The Spread of SARS-CoV-2 Variant Omicron with a Doubling Time of 2.0-3.3 Days Can Be Explained by Immune Evasion. *Viruses*, *14*(2). https://doi.org/10.3390/v14020294

Hadfield, J., Megill, C., Bell, S. M., Huddleston, J., Potter, B., Callender, C., Sagulenko, P., Bedford, T., & Neher, R. A. (2018). Nextstrain: real-time tracking of pathogen evolution. *Bioinformatics*, *34*(23), 4121-4123. https://doi.org/10.1093/bioinformatics/bty407

Harcourt, J., Tamin, A., Lu, X., Kamili, S., Sakthivel, S. K., Murray, J., Queen, K., Tao, Y., Paden, C. R., Zhang, J., Li, Y., Uehara, A., Wang, H., Goldsmith, C., Bullock, H. A., Wang, L., Whitaker, B., Lynch, B., Gautam, R., Schindewolf, C., Lokugamage, K. G., Scharton, D., Plante, J. A., Mirchandani, D., Widen, S. G., Narayanan, K., Makino, S., Ksiazek, T. G., Plante, K. S., Weaver, S. C., Lindstrom, S., Tong, S., Menachery, V. D., & Thornburg, N. J. (2020). Severe Acute Respiratory Syndrome Coronavirus 2 from Patient with Coronavirus Disease, United States. *Emerg Infect Dis*, *26*(6), 1266-1273. https://doi.org/10.3201/eid2606.200516

Harvey, W. T., Carabelli, A. M., Jackson, B., Gupta, R. K., Thomson, E. C., Harrison, E. M., Ludden, C., Reeve, R., Rambaut, A., Consortium, C.-G. U., Peacock, S. J., & Robertson, D. L. (2021). SARS-CoV-2 variants, spike mutations and immune escape. *Nat Rev Microbiol*, *19*(7), 409-424. https://doi.org/10.1038/s41579-021-00573-0

Heidari, M., Sayfouri, N., & Jafari, H. (2022). Consecutive Waves of COVID-19 in Iran: Various Dimensions and Probable Causes. *Disaster Med Public Health Prep*, 1-14. https://doi.org/10.1017/dmp.2022.45

Hong, Q., Han, W., Li, J., Xu, S., Wang, Y., Xu, C., Li, Z., Wang, Y., Zhang, C., Huang, Z., & Cong, Y. (2022). Molecular basis of receptor binding and antibody neutralization of Omicron. *Nature*. https://doi.org/10.1038/s41586-022-04581-9

Jones, T. C., Biele, G., Muhlemann, B., Veith, T., Schneider, J., Beheim-Schwarzbach, J., Bleicker, T., Tesch, J., Schmidt, M. L., Sander, L. E., Kurth, F., Menzel, P., Schwarzer, R., Zuchowski, M., Hofmann, J., Krumbholz, A., Stein, A., Edelmann, A., Corman, V. M., & Drosten, C. (2021). Estimating infectiousness throughout SARS-CoV-2 infection course. *Science*, *373*(6551). https://doi.org/10.1126/science.abi5273

Konings, F., Perkins, M. D., Kuhn, J. H., Pallen, M. J., Alm, E. J., Archer, B. N., Barakat, A., Bedford, T., Bhiman, J. N., Caly, L., Carter, L. L., Cullinane, A., de Oliveira, T., Druce, J., El Masry, I., Evans, R., Gao, G. F., Gorbalenya, A. E., Hamblion, E., Herring, B. L., Hodcroft, E., Holmes, E. C., Kakkar, M., Khare, S., Koopmans, M. P. G., Korber, B., Leite, J., MacCannell, D., Marklewitz, M., Maurer-Stroh, S., Rico, J. A. M., Munster, V. J., Neher, R., Munnink, B. O., Pavlin, B. I., Peiris, M., Poon, L., Pybus, O., Rambaut, A., Resende, P., Subissi, L., Thiel, V., Tong, S., van der Werf, S., von Gottberg, A., Ziebuhr, J., & Van Kerkhove, M. D. (2021). SARS-CoV-2 Variants of Interest and Concern naming scheme conducive for global discourse. *Nat Microbiol*, *6*(7), 821-823. https://doi.org/10.1038/s41564-021-00932-w

Korber, B., Fischer, W. M., Gnanakaran, S., Yoon, H., Theiler, J., Abfalterer, W., Hengartner, N., Giorgi, E. E., Bhattacharya, T., Foley, B., Hastie, K. M., Parker, M. D., Partridge, D.

G., Evans, C. M., Freeman, T. M., de Silva, T. I., Sheffield, C.-G. G., McDanal, C., Perez, L. G., Tang, H., Moon-Walker, A., Whelan, S. P., LaBranche, C. C., Saphire, E. O., & Montefiori, D. C. (2020). Tracking Changes in SARS-CoV-2 Spike: Evidence that D614G Increases Infectivity of the COVID-19 Virus. *Cell*, *182*(4), 812-827 e819. https://doi.org/10.1016/j.cell.2020.06.043

Kutter, J. S., de Meulder, D., Bestebroer, T. M., Lexmond, P., Mulders, A., Richard, M., Fouchier, R. A. M., & Herfst, S. (2021). SARS-CoV and SARS-CoV-2 are transmitted through the air between ferrets over more than one meter distance. *Nat Commun*, *12*(1), 1653. https://doi.org/10.1038/s41467-021-21918-6

Lednicky, J. A., Lauzard, M., Fan, Z. H., Jutla, A., Tilly, T. B., Gangwar, M., Usmani, M., Shankar, S. N., Mohamed, K., Eiguren-Fernandez, A., Stephenson, C. J., Alam, M. M., Elbadry, M. A., Loeb, J. C., Subramaniam, K., Waltzek, T. B., Cherabuddi, K., Morris, J. G., Jr., & Wu, C. Y. (2020). Viable SARS-CoV-2 in the air of a hospital room with COVID-19 patients. *Int J Infect Dis*, *100*, 476-482. https://doi.org/10.1016/j.ijid.2020.09.025

Neerukonda, S. N., Vassell, R., Lusvarghi, S., Wang, R., Echegaray, F., Bentley, L., Eakin, A. E., Erlandson, K. J., Katzelnick, L. C., Weiss, C. D., & Wang, W. (2021). SARS-CoV-2 Delta Variant Displays Moderate Resistance to Neutralizing Antibodies and Spike Protein Properties of Higher Soluble ACE2 Sensitivity, Enhanced Cleavage and Fusogenic Activity. *Viruses*, *13*(12). https://doi.org/10.3390/v13122485

O'Toole, A., Hill, V., Pybus, O. G., Watts, A., Bogoch, II, Khan, K., Messina, J. P., consortium, C.-G. U., Network for Genomic Surveillance in South, A., Brazil, U. K. C. G. N., Tegally, H., Lessells, R. R., Giandhari, J., Pillay, S., Tumedi, K. A., Nyepetsi, G., Kebabonye, M., Matsheka, M., Mine, M., Tokajian, S., Hassan, H., Salloum, T., Merhi, G., Koweyes, J., Geoghegan, J. L., de Ligt, J., Ren, X., Storey, M., Freed, N. E., Pattabiraman, C., Prasad, P., Desai, A. S., Vasanthapuram, R., Schulz, T. F., Steinbruck, L., Stadler, T., Swiss Viollier Sequencing, C., Parisi, A., Bianco, A., Garcia de Viedma, D., Buenestado-Serrano, S., Borges, V., Isidro, J., Duarte, S., Gomes, J. P., Zuckerman, N. S., Mandelboim, M., Mor, O., Seemann, T., Arnott, A., Draper, J., Gall, M., Rawlinson, W., Deveson, I., Schlebusch, S., McMahon, J., Leong, L., Lim, C. K., Chironna, M., Loconsole, D., Bal, A., Josset, L., Holmes, E., St George, K., Lasek-Nesselquist, E., Sikkema, R. S., Oude Munnink, B., Koopmans, M., Brytting, M., Sudha Rani, V., Pavani, S., Smura, T., Heim, A., Kurkela, S., Umair, M., Salman, M., Bartolini, B., Rueca, M., Drosten, C., Wolff, T., Silander, O., Eggink, D., Reusken, C., Vennema, H., Park, A., Carrington, C., Sahadeo, N., Carr, M., Gonzalez, G., Diego, S. A. S., National Virus Reference, L., Seq, C. S., Danish Covid-19 Genome, C., Communicable Diseases Genomic, N., Dutch National, S.-C.-s. p., Division of Emerging Infectious, D., de Oliveira, T., Faria, N., Rambaut, A., & Kraemer, M. U. G. (2021). Tracking the international spread of SARS-CoV-2 lineages B.1.1.7 and B.1.351/501Y-V2 with grinch. *Wellcome Open Res*, *6*, 121. https://doi.org/10.12688/wellcomeopenres.16661.2

Port, J. R., Yinda, C. K., Avanzato, V. A., Schulz, J. E., Holbrook, M. G., van Doremalen, N., Shaia, C., Fischer, R. J., & Munster, V. J. (2022). Increased small particle aerosol transmission of B.1.1.7 compared with SARS-CoV-2 lineage A in vivo. *Nat Microbiol*, *7*(2), 213-223. https://doi.org/10.1038/s41564-021-01047-y

Port, J. R., Yinda, C. K., Owusu, I. O., Holbrook, M., Fischer, R., Bushmaker, T., Avanzato, V. A., Schulz, J. E., Martens, C., van Doremalen, N., Clancy, C. S., & Munster, V. J. (2021). SARS-CoV-2 disease severity and transmission efficiency is increased for airborne compared to fomite exposure in Syrian hamsters. *Nat Commun*, *12*(1), 4985. https://doi.org/10.1038/s41467-021-25156-8

Qing, E., Kicmal, T., Kumar, B., Hawkins, G. M., Timm, E., Perlman, S., & Gallagher, T. (2021). Dynamics of SARS-CoV-2 Spike Proteins in Cell Entry: Control Elements in the Amino-Terminal Domains. *MBio*, *12*(4), e0159021. https://doi.org/10.1128/mBio.01590-21

Richard, M., Kok, A., de Meulder, D., Bestebroer, T. M., Lamers, M. M., Okba, N. M. A., Fentener van Vlissingen, M., Rockx, B., Haagmans, B. L., Koopmans, M. P. G., Fouchier, R. A. M., & Herfst, S. (2020). SARS-CoV-2 is transmitted via contact and via the air between ferrets. *Nat Commun*, *11*(1), 3496. https://doi.org/10.1038/s41467-020-17367-2

Rochman, N. D., Wolf, Y. I., Faure, G., Mutz, P., Zhang, F., & Koonin, E. V. (2021). Ongoing global and regional adaptive evolution of SARS-CoV-2. *Proc Natl Acad Sci U S A*, *118*(29). https://doi.org/10.1073/pnas.2104241118

Scheuch, G. (2020). Breathing Is Enough: For the Spread of Influenza Virus and SARS-CoV-2 by Breathing Only. *J Aerosol Med Pulm Drug Deliv*, *33*(4), 230-234. https://doi.org/10.1089/jamp.2020.1616

Schuit, M., Biryukov, J., Beck, K., Yolitz, J., Bohannon, J., Weaver, W., Miller, D., Holland, B., Krause, M., Freeburger, D., Williams, G., Wood, S., Graham, A., Rosovitz, M. J., Bazinet, A., Phillips, A., Lovett, S., Garcia, K., Abbott, E., Wahl, V., Ratnesar-Shumate, S., & Dabisch, P. (2021). The stability of an isolate of the SARS-CoV-2 B.1.1.7 lineage in aerosols is similar to three earlier isolates. *J Infect Dis*. https://doi.org/10.1093/infdis/jiab171

Sia, S. F., Yan, L. M., Chin, A. W. H., Fung, K., Choy, K. T., Wong, A. Y. L., Kaewpreedee, P., Perera, R., Poon, L. L. M., Nicholls, J. M., Peiris, M., & Yen, H. L. (2020). Pathogenesis and transmission of SARS-CoV-2 in golden hamsters. *Nature*, *583*(7818), 834-838. https://doi.org/10.1038/s41586-020-2342-5

Smither, S. J., Eastaugh, L. S., Findlay, J. S., & Lever, M. S. (2020). Experimental aerosol survival of SARS-CoV-2 in artificial saliva and tissue culture media at medium and high humidity. *Emerg Microbes Infect*, *9*(1), 1415-1417. https://doi.org/10.1080/22221751.2020.1777906

Tao, K., Tzou, P. L., Nouhin, J., Gupta, R. K., de Oliveira, T., Kosakovsky Pond, S. L., Fera, D., & Shafer, R. W. (2021). The biological and clinical significance of emerging SARS-CoV-2 variants. *Nat Rev Genet*, *22*(12), 757-773. https://doi.org/10.1038/s41576-021-00408-x

van Doremalen, N., Bushmaker, T., Morris, D. H., Holbrook, M. G., Gamble, A., Williamson, B. N., Tamin, A., Harcourt, J. L., Thornburg, N. J., Gerber, S. I., Lloyd-Smith, J. O., de Wit, E., & Munster, V. J. (2020). Aerosol and Surface Stability of SARS-CoV-2 as Compared with SARS-CoV-1. *N Engl J Med*, *382*(16), 1564-1567. https://doi.org/10.1056/NEJMc2004973

van Doremalen, N., Schulz, J. E., Adney, D. R., Saturday, T. A., Fischer, R. J., Yinda, C. K., Thakur, N., Newman, J., Ulaszewska, M., Belij-Rammerstorfer, S., Saturday, G., Spencer, A. J., Bailey, D., Gilbert, S. C., Lambe, T., & Munster, V. J. (2022). Efficacy of ChAdOx1 vaccines against SARS-CoV-2 Variants of Concern Beta, Delta and Omicron in the Syrian hamster model. *Res Sq*. https://doi.org/10.21203/rs.3.rs-1343927/v1

Vardhan, S., & Sahoo, S. K. (2022). Computational studies on the interaction of SARS-CoV-2 Omicron SGp RBD with human receptor ACE2, limonin and glycyrrhizic acid. *Comput Biol Med*, *144*, 105367. https://doi.org/10.1016/j.compbiomed.2022.105367

Wang, C. C., Prather, K. A., Sznitman, J., Jimenez, J. L., Lakdawala, S. S., Tufekci, Z., & Marr, L. C. (2021). Airborne transmission of respiratory viruses. *Science*, *373*(6558). https://doi.org/10.1126/science.abd9149

WHO Coronavirus (COVID-19) Dashboard. (2022, 5:18pm CET, 4 March 2022). https://covid19.who.int/

Wolf, K. A., Kwan, J. C., & Kamil, J. P. (2022). Structural Dynamics and Molecular Evolution of the SARS-CoV-2 Spike Protein. *MBio*, e0203021. https://doi.org/10.1128/mbio.02030-21

World Health Organization - Tracking SARS-CoV-2 variants. (2020-2022, 3 February 2022). https://www.who.int/en/activities/tracking-SARS-CoV-2-variants/

Yurkovetskiy, L., Wang, X., Pascal, K. E., Tomkins-Tinch, C., Nyalile, T. P., Wang, Y., Baum, A., Diehl, W. E., Dauphin, A., Carbone, C., Veinotte, K., Egri, S. B., Schaffner, S. F., Lemieux, J. E., Munro, J. B., Rafique, A., Barve, A., Sabeti, P. C., Kyratsous, C. A., Dudkina, N. V., Shen, K., & Luban, J. (2020). Structural and Functional Analysis of the D614G SARS-CoV-2 Spike Protein Variant. *Cell*, *183*(3), 739-751 e738. https://doi.org/10.1016/j.cell.2020.09.032

Zhang, C., Guo, Z., Zhao, Z., Wang, T., Li, L., Miao, F., Zhang, C., Li, Y., & Gao, Y. (2021). SARS-CoV-2 Aerosol Exhaled by Experimentally Infected Cynomolgus Monkeys. *Emerg Infect Dis*, *27*(7), 1979-1981. https://doi.org/10.3201/eid2707.203948

Zhang, J., Cai, Y., Xiao, T., Lu, J., Peng, H., Sterling, S. M., Walsh, R. M., Jr., Rits-Volloch, S., Zhu, H., Woosley, A. N., Yang, W., Sliz, P., & Chen, B. (2021). Structural impact on SARS-CoV-2 spike protein by D614G substitution. *Science*, *372*(6541), 525-530. https://doi.org/10.1126/science.abf2303

CHAPTER FOUR

DISCUSSION

Completion of the second anniversary of the SARS-CoV-2 pandemic, public health is facing a continuation of many unknowns and successive waves. A retrospective look at December 2019 to January 2020, a cluster of patients in Hubei Providence of China began to experience an unknown etiology with symptoms of pneumonia. The first 425 cases were described and linked to the Huanan Seafood Wholesale Market in Wuhan, with additional cases that had not been related [28]. Of all the cases, 55% had disease onset before January 1, 2020, suggestive of onset starting in early December. With this data it was estimated that R_0 was 2.2 for the unknown etiology named 2019 novel coronavirus (2019-nCoV) at that time [28].

During the stochastic phase of the pandemic, the general knowledge of transmission was still unknown. With the initial confirmed findings of the ACE2 receptor of SARS-CoV-2 by our group, along with a 79% similarity to the original SARS-CoV-1, it was speculated that aerosol and/or fomite transmission could be important [65, 66]. In our initial study, we looked at the fomite and aerosol stability of the SARS-CoV-2 nCoV-WA1-2020 (MN985325.1) versus the original SARS-CoV-1 Tor2 (AY274119.3) isolate. In the fomite study, we were able to closely replicate the cycle-threshold values (20 -22 Ct) from samples obtained by others for the upper and lower respiratory tract in humans with an inoculum of 10^5 $TCID_{50}$/mL for both viruses [67]. The results concluded that copper, stainless steel and plastic surfaces had a similar half-life while cardboard had the biggest variation (Chapter 2- Figure 1). In the aerosol experiments, the inoculum was $10^{6.75\text{-}7.00}$ $TCID_{50}$/mL for SARS-CoV-1 and $10^{5.25}$ $TCID_{50}$/mL for SARS-CoV-2. The highest titer inoculum was required because the decay reduction of infectious titer and

duration of viability was unknown. The aerosol viability was observed during the duration of multi-sampling events of the experiment (≤ 3hours) with a half-life of 1.18 for SARS-CoV-1 and 1.09 for SARS-CoV-2. These findings suggest that aerosol and fomite transmission were plausible routes of transmission for SARS-CoV-2; with minimum difference from SARS-CoV-1.

Still in the initial phase in January 2020, the World Health Organization (WHO), in collaboration with other entities, began to monitor for signs of evolution of SARS-CoV-2. In late 2020, mutations in the genomic sequence started to emerge with a population level health impact. On May 31, 2021, a panel of scientists from the WHO Virus Evolution Working Group (now called the Technical Advisory Group on Virus Evolution) established a nomenclature system for naming and tracking Variants of Interest (VOIs) and Variants of Concern (VOCs) [38, 53]. WHO established a naming system for VOIs and VOCs using the Greek alphabet (e.g., Alpha, Beta, etc.). In addition, a second naming process was developed for tracking in relation to phylogenetic classification. The Phylogenetic Assignment of Named Global Outbreak (PANGO) lineages, in collaboration with NextStrain, is used with a delineated letter prefix followed by a number(s) to track the mutational lineages (e.g., B.1.1.7) [52]. The second PANGO system has limitations in regard to sub-lineages, but still provides the best differentiation tracking method [45]. Now with established pandemic nomenclator, real-time sequencing and tracking can be followed.

In December 2021, a review by Tao et al. was able to discuss the biological and clinical significance of SARS-CoV-2 for the ancestral strains and VOCs including Wuhan- Hu-1, B.1(D614G), B.1.1.7 (Alpha), B.1.351(Beta), Gamma (P.1), and B.1.617.2 (Delta) [54]. The research showed that during the early months of the pandemic, SARS-CoV-2 was adapting to

increased efficiency in human-to-human transmission. The emergence of new VOCs with increased transmission, disease severity, and humoral immunity escape prompted continual monitoring. Additional concerns arose with production of therapeutic medication efficiency, established diagnostic tools, and public health and social measures that were being administrated.

After this initial phase, along with the continued evolving SARS-CoV-2 genome, it highlighted the importance to look at the mechanisms used by coronaviruses for proofreading. The nonstructural protein 14 (nsp14) is the exoribonuclease enzyme used by SARS- COV-1 for this proofreading function and is the same mechanism used by SARS-CoV-2 [68]. The exonuclease enzyme has been shown to reduce replicated error 15-20-fold in *in vivo* models. However, the virus can still acquire these drift point mutations demonstrated by the emergence of VOCs. This ability to fix genomic mutation is important because coronaviruses, and importantly SARS-CoV-2, can acquire shift mutations through recombination with two co-infection viruses (e.g., Delta-Omicron (AY.4/BA.1)-EPI_ISL_10819657) [69]. The recombination method of evolution is the proposed reason for SARS-CoV-2 spillover, with a melting pot of coronaviruses in bats populations, and the continued evolution and rise of VOCs during the pandemic [70].

The SARS-CoV-2 index variant evolved from the original ancestral strain Wuhan- Hu-1 with a point mutation in the spike region of D614G. The mutation was retrospectively found to have arisen in early 2020. Another variant with the D614G mutation became the new dominate virus B.1.1.7 (Alpha), rising in September - December 2020 in the United Kingdom. The proposed advantage of the mutation is that major evolutionary selective pressures required the increased efficiency of binding to the angiotensin converting enzyme 2 (ACE2). In the

discussion section of Chapter 3 we propose the increase binding likely had a direct effect on transmission by lowering the infectious dose. This D614G mutation was studied in detail in the VOC stability manuscript (Chapter 3 - Figure 1 & 2). In conclusion, it suggests that SARS-CoV-2 aerosol stability is dependent on efficiency of the ACE2 binding, enhanced with TMPRESS2 activation, and is likely dependent on viral entry for these VOC isolates: B.1, Alpha, Beta, and Delta (Chapter 3 - Figure 1D & Figure 2).

This cell-surface mediated mechanisms of the spike binding to ACE2 receptor, with the cleavage by TMPRESS2, for coronavirus entry, have been studied and described [71, 72]. Briefly explained, a prefusion conformation of S engages with host cell receptors and undergoes proteolytic processing to reach a fusion-competent state. The fusion proteins gather (S1 and S2) to make a two-domain system in an un-cleaved trimer formation. The S1 binds with the host cell, with the ACE2 receptor, while acting as the chaperone for the S2 protein. The S2 has a spring-loaded mechanism, when cut by a protease cleavage (e.g., TMPRSS2) it preforms the attachment of membrane fusion. The cleavage at the junction of the S1/S2 provides the machinery to change confirmation; to allow for quick entry on the cell surface [73]. The “quick fusogenicity” may explain the faster aerosol transmission by Delta [74]. Whereas, it has been suggested that Omicron has attenuated fusogenicity and pathogenicity in comparison to Delta [75]. Omicron’s transmission ability may have opted for endocytosis entry over the cell surface fusion method; this proposition supports the idea that Omicron is less infectious to the lung cells while retraining the ability to transmit at a population level [76]. These studies are consistent with our viral entry data in Chapter 3 - Figure 1D.

The importance of the preprocessing loading or priming in an open conformation by proprotein convertase furin (aka furin cleave site) has been demonstrated [77]. This suggests the furin site is a crucial component for the success of SARS-CoV-2. With the "open conformation", showing 1 - 3 of the S trimers in the up position, the P681H/R mutations allow the proteolytic process to be more efficient. Compounding the effect with the presence of cell surface proteases TMPRSS2; this enhances the process of entry on the cell surface fusion. The addition of the D614G substitution and RBD mutations such as N501Y and E484K likewise increase the RBD opening, which would promote the binding to ACE2. These changes would allow for quicker entry by allowing S2' exposure to the proteases [39]. With cleavage of the S2' the virus can move to a post-fusion state with the target cell.

The proposed "open conformation" of the S trimers, by Wolf et al, suggest this would be important for a seronegative population that would allow for quick entry with higher transmission. This would suggest at the initial phase of the pandemic for the circulation of the WA1 strain, with R_0 2-5, the confirmation would be a "closed" RBD confirmation. The evolution from alpha-to-beta-to-delta leading to an increase in transmission rates (arriving at R_t ~7) suggests an open confirmation. However, it has been suggested that Omicron's Rt could be around 10; during the UK outbreak, there was a doubling of cases every 2-3 days [78]. While the higher $Rt_{\#}$ of Omicron suggests a "open RBD" leading to an increase chance of binding, a contradiction is suggested of a "closed" confirmation for Omicron [39]. With the contradiction, a little more in-depth view of the increase in seropositive population after 2 years of pandemic exposure, it can see the suggested "closed" protective confirmation. This supports the narrative

for Omicron's ability of humoral immune evasion, while increasing transmission, as the leading driver of the emergence.

For infection within a serological positive population the virus will need to escape the presence of humoral immunity from vaccination or natural infection. Wolf et al. highlighted a "Canyon Hypothesis" proposed by M.G. Rossmann stating, "The canyon's surface is inaccessible to the broad antigen binding region of antibodies, permitting conservation of residues that might be required for host cell receptor recognition without danger of attack by the host's immune system. In contrast, the exposed surface features, where neutralizing antibodies are known to bind, change rapidly under pressure from the host's immune system."[79]. Rossman (1989), confirmed this for human rhinovirus 14 and similarly for influenza, both of which are airborne respiratory viruses like SARS-CoV-2. In addition, given the increasing rapid change of mutations (plasticity) of SARS-CoV-2 at the upper S1 region, the Canyon Hypothesis of evasion of the host's immune system is likely.

With the proposed subvariant of Omicron, the BA.2 suggests a more closed RBD as an evolutionary shift from the Beta variant's open RBD. For instance, a variant like Omicron with a less fusogenic spike may be more transmissible despite having lower titers if it is less likely to misfire (remaining stable) before reaching a new host during aerosol transmission. The ability to remain hidden from the host's immune system once it reaches the new host also promotes transmission. By contrast, a variant like Beta with a more fusogenic spike can be more transmissible if it overcomes the drawbacks of instability through rapid growth kinetics, high titers, tissue tropism, and/or density dependent transmission [39].

In Chapter 3, regarding the current circulating strain Omicron BA.1, we suggest the attenuated viral entry and aerosol stability is an exchange for the enhanced ability for immune escape. These characteristics of the closed RBD, with the Canyon Hypothesis, might parallel the suggested increase in fomite transmission stability by preventing misfiring or degradation of the spike S1/S2 region. In contrast to the decreasing aerosol stability of Delta and Omicron in Chapter 3, the fomite stability has been suggested to have a increasing linear progression for these two variants. The paper states, "Specifically, survival times of the Wuhan strain, Alpha variant, Beta variant, Gamma variant, Delta variant, and Omicron variant on skin surfaces were 8.6 h (95% CI, 6.5–10.9 h), 19.6 h (95% CI, 14.8–25.3 h), 19.1 h (95% CI, 13.9– 25.3 h), 11.0 h (95% CI, 8.1–14.7 h), 16.8 h (95% CI, 13.1–21.1 h), and 21.1 h (95% CI, 15.8– 27.6 h), respectively." An important factor to consider is the physiochemistry differences between fomite droplets, with larger and more stable composition, then of the aerosol droplet nuclei's desiccation. The paper proposes for the fomite transmission, "Additionally, the Omicron variant might have been replaced by the Delta variant due to its increased environmental stability and rapid spread". Whereas fomite might be a compounding factor, with immune escape, no evidence suggests fomite transmission as a driving factor of the current phase of the pandemic [80-82].

As Omicron BA.1 looks to be conceding to the subvariant BA.2, along with additional developments of recombinant variants like Delta - Omicron BA.4, continuation of aerosol and fomite studies are warranted. The lineage of Omicron BA.1 peaked in late January 2022 while another wave of cases of BA.2 is gaining momentum in Europe and Asian counties.

The Omicron subvariants have been a surprise with the ability of immune evasion and reduction of vaccine efficacy [78, 83]. Currently the BA.1 is the current circulating strain that has been the most widespread VOC to date but looks to be replaced. The BA.2 has been less productive to date but has been reported to have 2.62 odds of transmission compared to BA.1 in unvaccinated individuals; this increase in transmission is not observed (odds ratio =1) in fully or boosted individuals [84]. This increase in transmissibility of BA.1 is surprising since the nasal shedding does not seem to surpass the nasal shedding of the Delta variant [85, 86]. Furthermore, the affinity binding of the spike of BA.1 to the human ACE2 is only twice (~2.4) as robust as the original WA1; similar to the entry data of a 2.97 fold increase from WA1 to B.1. With the increase in transmissibility of BA.1, without increase shedding, we should be looking at similar entry as the ancestral B.1 in entry data (Chapter 3- Figure 1D). However, BA.2 will be surprising because of the suspected enhancement to evade antibody mediated immunity [87]. In conclusion, BA.2 will probably need to demonstrate an increase in entry with a more "open" S trimer confirmation to overtake BA.1 without trading-off the immune evasion phenotype.

With the ever-changing finish line of the SARS-CoV-2 pandemic, the continuous monitoring of SARS-CoV-2 evolution by the fields of public health, phenotypic biology, and aerobiology need to remain vigilant during subsequent waves of emerging VOCs and subvariants.

CHAPTER FIVE

CONCLUSION

With the fluid situation of the COVID-19 pandemic occurring during modern times, the increased ability of communication has provided platforms to follow vital information in real-time. Platforms for preprint servers, pathogen genome data, and daily metrics on COVID cases, mortality, and vaccination rates have all been developed for real-time analysis. From the first notification of an "UNDIAGNOSED PNEUMONIA - CHINA (HUBEI): REQUEST FOR INFORMATION Published Date: 2019-12-30 18:59:00 EST" on Promedmail.org, the public health sector was able to follow the progression of the outbreak [88]. Once the SARS-CoV-2 sequencing was publicly posted in early January 2020, Letko et al. was able to confirm the ACE2 cell receptor (by January 22, 2020 in preprint) [65]. On March 13, 2020, the co-first author manuscript comparing SARS-CoV-1 to SARS-CoV-2 aerosol and fomite stability was available in preprint at medRxiv (Chapter 2) [89]. With additional concern about supply chain issues of N95 respirators and protection of hospital personnel; the decontamination and re-use of the N95s was answered in a preprint on April 24,2020 at medRxiv [90]. Most importantly, by May 13, 2020 the immunogenicity information for the non-human primate model was in preprint at bioRxiv for the human approved Oxford/AstraZeneca (ChAdOx1-S [recombinant]) COVID-19 vaccine [91]. With the expediency of the information we provided, public health experts were able to develop non-pharmacological interventions while therapeutics and vaccines were still in development.

In the next phase of the pandemic, we tested the K18-hACE2 mouse model, with other co-first authors, to develop a lethal animal model for testing pathogenesis and medical

countermeasure [92]. In concurrent investigation with vaccine efficacy studies, the next generation of COVID-19 vaccines was in development, we were part of testing routes of vaccination for better mucosal immunity and reduced viral shedding along with others [16, 93].

In this current phase of the pandemic (late 2021 - early 2022) our aerosolization studies and modelling are timely with the emergence of new VOCs [18, 94]. Throughout the pandemic I have provided, with others, the knowledge to fill in the gaps of the unknowns of SARS-CoV-2. As the major method of the transmission for SARS-CoV-2, with the ability to cause superspreader events, the aerosol route and stability will require continued surveillance. Subsets of these studies may prove to be limited in the future unless a dramatic change in SARS-CoV-2 epidemiology or natural history of the virus evolves causing a major shift. Investigation of environmental persistence and mechanistic studies seem to be finite, nevertheless the situation will need to be monitored for changes in VOC emergence. Additional inquiries for next generation mucosal vaccines, therapeutics, and prophylactics for protection against SARS-CoV-2 bioaerosol will become the primary objective of pandemic aerobiologist [95].

CUMULATIVE LITERATURE CITED

1. Sia, S.F., L.M. Yan, A.W.H. Chin, K. Fung, K.T. Choy, A.Y.L. Wong, P. Kaewpreedee, R. Perera, L.L.M. Poon, J.M. Nicholls, M. Peiris, and H.L. Yen, *Pathogenesis and transmission of SARS-CoV-2 in golden hamsters.* Nature, 2020. **583**(7818): p. 834-838 DOI: 10.1038/s41586-020-2342-5.

2. Hartman, A.L., S. Nambulli, C.M. McMillen, A.G. White, N.L. Tilston-Lunel, J.R. Albe, E. Cottle, M.D. Dunn, L.J. Frye, T.H. Gilliland, E.L. Olsen, K.J. O'Malley, M.M. Schwarz, J.A. Tomko, R.C. Walker, M. Xia, M.S. Hartman, E. Klein, C.A. Scanga, J.L. Flynn, W.B. Klimstra, A.K. McElroy, D.S. Reed, and W.P. Duprex, *SARS-CoV-2 infection of African green monkeys results in mild respiratory disease discernible by PET/CT imaging and shedding of infectious virus from both respiratory and gastrointestinal tracts.* PLoS Pathog, 2020. **16**(9): p. e1008903 DOI: 10.1371/journal.ppat.1008903.

3. Coleman, K.K., D.J.W. Tay, K. Sen Tan, S.W.X. Ong, T.T. Son, M.H. Koh, Y.Q. Chin, H. Nasir, T.M. Mak, J.J.H. Chu, D.K. Milton, V.T.K. Chow, P.A. Tambyah, M. Chen, and T.K. Wai, *Viral Load of SARS-CoV-2 in Respiratory Aerosols Emitted by COVID-19 Patients while Breathing, Talking, and Singing.* Clin Infect Dis, 2021 DOI: 10.1093/cid/ciab691.

4. Hu, B., H. Guo, P. Zhou, and Z.L. Shi, *Characteristics of SARS-CoV-2 and COVID-19.* Nat Rev Microbiol, 2021. **19**(3): p. 141-154 DOI: 10.1038/s41579-020-00459-7.

5. Braden, C.R., S.F. Dowell, D.B. Jernigan, and J.M. Hughes, *Progress in global surveillance and response capacity 10 years after severe acute respiratory syndrome.* Emerg Infect Dis, 2013. **19**(6): p. 864-9 DOI: 10.3201/eid1906.130192.

6. Zaki, A.M., S. van Boheemen, T.M. Bestebroer, A.D. Osterhaus, and R.A. Fouchier, *Isolation of a novel coronavirus from a man with pneumonia in Saudi Arabia.* N Engl J Med, 2012. **367**(19): p. 1814-20 DOI: 10.1056/NEJMoa1211721.

7. van Doremalen, N., Z.S. Hijazeen, P. Holloway, B. Al Omari, C. McDowell, D. Adney, H.A. Talafha, J. Guitian, J. Steel, N. Amarin, M. Tibbo, E. Abu-Basha, A.M. Al-Majali, V.J. Munster, and J.A. Richt, *High Prevalence of Middle East Respiratory Coronavirus in Young Dromedary Camels in Jordan.* Vector Borne Zoonotic Dis, 2017. **17**(2): p. 155-159 DOI: 10.1089/vbz.2016.2062.

8. Kim, K.H., T.E. Tandi, J.W. Choi, J.M. Moon, and M.S. Kim, *Middle East respiratory syndrome coronavirus (MERS-CoV) outbreak in South Korea, 2015: epidemiology, characteristics and public health implications.* J Hosp Infect, 2017. **95**(2): p. 207-213 DOI: 10.1016/j.jhin.2016.10.008.

9. Goldberg, L.J., H.M.S. Watkins, E.E. Boerke, and M.A. Chatigny, *The Use of a Rotating Drum for the Study of Aerosols over Extended Periods of Time.* American Journal of Hygiene, 1958. **68**(1): p. 85-93 DOI: DOI 10.1093/oxfordjournals.aje.a119954.

10. van Doremalen, N., M. Letko, R.J. Fischer, T. Bushmaker, J. Schulz, C.K. Yinda, S.N. Seifert, N.J. Kim, M.G. Hemida, G. Kayali, W.B. Park, R. Perera, A. Tamin, N.J. Thornburg, S. Tong, K. Queen, M.D. van Kerkhove, Y.K. Choi, M.D. Oh, A.M. Assiri, M. Peiris, S.I. Gerber, and V.J. Munster, *SurfaceAerosol Stability and Pathogenicity of Diverse Middle East Respiratory Syndrome Coronavirus Strains, 20122018.* Emerg Infect Dis, 2021. **27**(12): p. 3052-3062 DOI: 10.3201/eid2712.210344.

11. Badawi, A. and S.G. Ryoo, *Prevalence of comorbidities in the Middle East respiratory syndrome coronavirus (MERS-CoV): a systematic review and meta-analysis.* Int J Infect Dis, 2016. **49**: p. 129-33 DOI: 10.1016/j.ijid.2016.06.015.

12. Speranza, E., J.N. Purushotham, J.R. Port, B. Schwarz, M. Flagg, B.N. Williamson, F. Feldmann, M. Singh, L. Perez-Perez, G.L. Sturdevant, L.M. Roberts, A. Carmody, J.E. Schulz, N. van Doremalen, A. Okumura, J. Lovaglio, P.W. Hanley, C. Shaia, R.N. Germain, S.M. Best, V.J. Munster, C.M. Bosio, and E. de Wit, *Age-related differences in immune dynamics during SARS-CoV-2 infection in rhesus macaques.* Life Sci Alliance, 2022. **5**(4) DOI: 10.26508/lsa.202101314.

13. Port, J.R., D.R. Adney, B. Schwarz, J.E. Schulz, D.E. Sturdevant, B.J. Smith, V.A. Avanzato, M.G. Holbrook, J.N. Purushotham, K.A. Stromberg, I. Leighton, C.M. Bosio, C. Shaia, and V.J. Munster, *High-Fat High-Sugar Diet-Induced Changes in the Lipid Metabolism Are Associated with Mildly Increased COVID-19 Severity and Delayed Recovery in the Syrian Hamster.* Viruses, 2021. **13**(12) DOI: 10.3390/v13122506.

14. Cruciata, A., L. Volpicelli, S. Di Bari, G. Iaiani, B. Cirillo, F. Pugliese, D. Pellegrino, G. Galardo, and G. Taliani, *Risk of Seven-Day Worsening and Death: A New Clinically Derived COVID-19 Score.* Viruses, 2022. **14**(3) DOI: 10.3390/v14030642.

15. Holloway, P., M. Gibson, N. van Doremalen, S. Nash, T. Holloway, M. Letko, J.M. Cardwell, B. Al Omari, A. Al-Majali, E. Abu-Basha, P. Mangtani, V.J. Munster, and J.

Guitian, *Risk Factors for Middle East Respiratory Syndrome Coronavirus Infection among Camel Populations, Southern Jordan, 2014-2018.* Emerg Infect Dis, 2021. **27**(9): p. 2301-2311 DOI: 10.3201/eid2709.203508.

16. Bold, D., N. van Doremalen, O. Myagmarsuren, B. Zayat, V.J. Munster, and J.A. Richt, *Middle East Respiratory Syndrome-Coronavirus Seropositive Bactrian Camels, Mongolia.* Vector Borne Zoonotic Dis, 2021. **21**(2): p. 128-131 DOI: 10.1089/vbz.2020.2669.

17. Lytras, S., W. Xia, J. Hughes, X. Jiang, and D.L. Robertson, *The animal origin of SARS-CoV-2.* Science, 2021. **373**(6558): p. 968-970 DOI: 10.1126/science.abh0117.

18. Port, J.R., C.K. Yinda, I.O. Owusu, M. Holbrook, R. Fischer, T. Bushmaker, V.A. Avanzato, J.E. Schulz, C. Martens, N. van Doremalen, C.S. Clancy, and V.J. Munster, *SARS-CoV-2 disease severity and transmission efficiency is increased for airborne compared to fomite exposure in Syrian hamsters.* Nat Commun, 2021. **12**(1): p. 4985 DOI: 10.1038/s41467-021-25156-8.

19. Adney, D.R., N. van Doremalen, V.R. Brown, T. Bushmaker, D. Scott, E. de Wit, R.A. Bowen, and V.J. Munster, *Replication and shedding of MERS-CoV in upper respiratory tract of inoculated dromedary camels.* Emerg Infect Dis, 2014. **20**(12): p. 1999-2005 DOI: 10.3201/eid2012.141280.

20. van Doremalen, N., T. Lambe, A. Spencer, S. Belij-Rammerstorfer, J.N. Purushotham, J.R. Port, V.A. Avanzato, T. Bushmaker, A. Flaxman, M. Ulaszewska, F. Feldmann, E.R. Allen, H. Sharpe, J. Schulz, M. Holbrook, A. Okumura, K. Meade-White, L. Perez-Perez, N.J. Edwards, D. Wright, C. Bissett, C. Gilbride, B.N. Williamson, R. Rosenke, D. Long, A. Ishwarbhai, R. Kailath, L. Rose, S. Morris, C. Powers, J. Lovaglio, P.W. Hanley, D. Scott, G. Saturday, E. de Wit, S.C. Gilbert, and V.J. Munster, *ChAdOx1 nCoV-19 vaccine prevents SARS-CoV-2 pneumonia in rhesus macaques.* Nature, 2020. **586**(7830): p. 578-582 DOI: 10.1038/s41586-020-2608-y.

21. van Doremalen, N., E. Haddock, F. Feldmann, K. Meade-White, T. Bushmaker, R.J. Fischer, A. Okumura, P.W. Hanley, G. Saturday, N.J. Edwards, M.H.A. Clark, T. Lambe, S.C. Gilbert, and V.J. Munster, *A single dose of ChAdOx1 MERS provides protective immunity in rhesus macaques.* Sci Adv, 2020. **6**(24): p. eaba8399 DOI: 10.1126/sciadv.aba8399.

22. Fischer, R., S. Judson, K. Miazgowicz, T. Bushmaker, J. Prescott, and V.J. Munster, *Ebola Virus Stability on Surfaces and in Fluids in Simulated Outbreak Environments.* Emerg Infect Dis, 2015. **21**(7): p. 1243-6 DOI: 10.3201/eid2107.150253.

23. van Doremalen, N., T. Bushmaker, D.H. Morris, M.G. Holbrook, A. Gamble, B.N. Williamson, A. Tamin, J.L. Harcourt, N.J. Thornburg, S.I. Gerber, J.O. Lloyd-Smith, E. de Wit, and V.J. Munster, *Aerosol and Surface Stability of SARS-CoV-2 as Compared with SARS-CoV-1*. N Engl J Med, 2020. **382**(16): p. 1564-1567 DOI: 10.1056/NEJMc2004973.

24. Fischer, R.J., T. Bushmaker, S. Judson, and V.J. Munster, *Comparison of the Aerosol Stability of 2 Strains of Zaire ebolavirus From the 1976 and 2013 Outbreaks.* J Infect Dis, 2016. **214**(suppl 3): p. S290-S293 DOI: 10.1093/infdis/jiw193.

25. Fischer, R.J., S. Judson, K. Miazgowicz, T. Bushmaker, and V.J. Munster, *Ebola Virus Persistence in Semen Ex Vivo.* Emerg Infect Dis, 2016. **22**(2): p. 289-91 DOI: 10.3201/eid2202.151278.

26. Prescott, J., T. Bushmaker, R. Fischer, K. Miazgowicz, S. Judson, and V.J. Munster, *Postmortem stability of Ebola virus.* Emerg Infect Dis, 2015. **21**(5): p. 856-9 DOI: 10.3201/eid2105.150041.

27. Matson, M.J., C.K. Yinda, S.N. Seifert, T. Bushmaker, R.J. Fischer, N. van Doremalen, J.O. Lloyd-Smith, and V.J. Munster, *Effect of Environmental Conditions on SARS-CoV-2 Stability in Human Nasal Mucus and Sputum*. Emerg Infect Dis, 2020. **26**(9) DOI: 10.3201/eid2609.202267.

28. Li, Q., X. Guan, P. Wu, X. Wang, L. Zhou, Y. Tong, R. Ren, K.S.M. Leung, E.H.Y. Lau, J.Y. Wong, X. Xing, N. Xiang, Y. Wu, C. Li, Q. Chen, D. Li, T. Liu, J. Zhao, M. Liu, W. Tu, C. Chen, L. Jin, R. Yang, Q. Wang, S. Zhou, R. Wang, H. Liu, Y. Luo, Y. Liu, G. Shao, H. Li, Z. Tao, Y. Yang, Z. Deng, B. Liu, Z. Ma, Y. Zhang, G. Shi, T.T.Y. Lam, J.T. Wu, G.F. Gao, B.J. Cowling, B. Yang, G.M. Leung, and Z. Feng, *Early Transmission Dynamics in Wuhan, China, of Novel Coronavirus-Infected Pneumonia.* N Engl J Med, 2020. **382**(13): p. 1199-1207 DOI: 10.1056/NEJMoa2001316.

29. Lednicky, J.A., M. Lauzard, Z.H. Fan, A. Jutla, T.B. Tilly, M. Gangwar, M. Usmani, S.N. Shankar, K. Mohamed, A. Eiguren-Fernandez, C.J. Stephenson, M.M. Alam, M.A. Elbadry, J.C. Loeb, K. Subramaniam, T.B. Waltzek, K. Cherabuddi, J.G. Morris, Jr., and

C.Y. Wu, *Viable SARS-CoV-2 in the air of a hospital room with COVID-19 patients.* Int J Infect Dis, 2020. **100**: p. 476-482 DOI: 10.1016/j.ijid.2020.09.025.

30. Adenaiye, O.O., J. Lai, P.J.B. de Mesquita, F. Hong, S. Youssefi, J. German, S.S. Tai, B. Albert, M. Schanz, S. Weston, J. Hang, C. Fung, H.K. Chung, K.K. Coleman, N. Sapoval, T. Treangen, I.M. Berry, K. Mullins, M. Frieman, T. Ma, D.K. Milton, and C.R.G. University of Maryland Stop, *Infectious SARS-CoV-2 in Exhaled Aerosols and Efficacy of Masks During Early Mild Infection.* Clin Infect Dis, 2021 DOI: 10.1093/cid/ciab797.

31. Zhang, C., Z. Guo, Z. Zhao, T. Wang, L. Li, F. Miao, C. Zhang, Y. Li, and Y. Gao, *SARS-CoV-2 Aerosol Exhaled by Experimentally Infected Cynomolgus Monkeys.* Emerg Infect Dis, 2021. **27**(7): p. 1979-1981 DOI: 10.3201/eid2707.203948.

32. Kutter, J.S., D. de Meulder, T.M. Bestebroer, P. Lexmond, A. Mulders, M. Richard, R.A.M. Fouchier, and S. Herfst, *SARS-CoV and SARS-CoV-2 are transmitted through the air between ferrets over more than one meter distance.* Nat Commun, 2021. **12**(1): p. 1653 DOI: 10.1038/s41467-021-21918-6.

33. Richard, M., A. Kok, D. de Meulder, T.M. Bestebroer, M.M. Lamers, N.M.A. Okba, M. Fentener van Vlissingen, B. Rockx, B.L. Haagmans, M.P.G. Koopmans, R.A.M. Fouchier, and S. Herfst, *SARS-CoV-2 is transmitted via contact and via the air between ferrets.* Nat Commun, 2020. **11**(1): p. 3496 DOI: 10.1038/s41467-020-17367-2.

34. Wang, C.C., K.A. Prather, J. Sznitman, J.L. Jimenez, S.S. Lakdawala, Z. Tufekci, and L.C. Marr, *Airborne transmission of respiratory viruses.* Science, 2021. **373**(6558) DOI: 10.1126/science.abd9149.

35. Fears, A.C., W.B. Klimstra, P. Duprex, A. Hartman, S.C. Weaver, K.S. Plante, D. Mirchandani, J.A. Plante, P.V. Aguilar, D. Fernandez, A. Nalca, A. Totura, D. Dyer, B. Kearney, M. Lackemeyer, J.K. Bohannon, R. Johnson, R.F. Garry, D.S. Reed, and C.J. Roy, *Persistence of Severe Acute Respiratory Syndrome Coronavirus 2 in Aerosol Suspensions.* Emerg Infect Dis, 2020. **26**(9) DOI: 10.3201/eid2609.201806.

36. Schuit, M., J. Biryukov, K. Beck, J. Yolitz, J. Bohannon, W. Weaver, D. Miller, B. Holland, M. Krause, D. Freeburger, G. Williams, S. Wood, A. Graham, M.J. Rosovitz, A. Bazinet, A. Phillips, S. Lovett, K. Garcia, E. Abbott, V. Wahl, S. Ratnesar-Shumate, and P. Dabisch, *The stability of an isolate of the SARS-CoV-2 B.1.1.7 lineage in aerosols is similar to three earlier isolates.* J Infect Dis, 2021 DOI: 10.1093/infdis/jiab171.

37. Heidari, M., N. Sayfouri, and H. Jafari, *Consecutive Waves of COVID-19 in Iran: Various Dimensions and Probable Causes.* Disaster Med Public Health Prep, 2022: p. 1-14 DOI: 10.1017/dmp.2022.45.

38. *World Health Organization - Tracking SARS-CoV-2 variants*. 2020-2022 3 February 2022; Available from: https://www.who.int/en/activities/tracking-SARS-CoV-2-variants/.

39. Wolf, K.A., J.C. Kwan, and J.P. Kamil, *Structural Dynamics and Molecular Evolution of the SARS-CoV-2 Spike Protein.* mBio, 2022: p. e0203021 DOI: 10.1128/mbio.02030-21.

40. Corman, V.M., O. Landt, M. Kaiser, R. Molenkamp, A. Meijer, D.K. Chu, T. Bleicker, S. Brunink, J. Schneider, M.L. Schmidt, D.G. Mulders, B.L. Haagmans, B. van der Veer, S. van den Brink, L. Wijsman, G. Goderski, J.L. Romette, J. Ellis, M. Zambon, M. Peiris, H. Goossens, C. Reusken, M.P. Koopmans, and C. Drosten, *Detection of 2019 novel coronavirus (2019-nCoV) by real-time RT-PCR.* Euro Surveill, 2020. **25**(3) DOI: 10.2807/1560-7917.ES.2020.25.3.2000045.

41. Port, J.R., C.K. Yinda, V.A. Avanzato, J.E. Schulz, M.G. Holbrook, N. van Doremalen, C. Shaia, R.J. Fischer, and V.J. Munster, *Increased small particle aerosol transmission of B.1.1.7 compared with SARS-CoV-2 lineage A in vivo.* Nat Microbiol, 2022. **7**(2): p. 213-223 DOI: 10.1038/s41564-021-01047-y.

42. Harcourt, J., A. Tamin, X. Lu, S. Kamili, S.K. Sakthivel, J. Murray, K. Queen, Y. Tao, C.R. Paden, J. Zhang, Y. Li, A. Uehara, H. Wang, C. Goldsmith, H.A. Bullock, L. Wang, B. Whitaker, B. Lynch, R. Gautam, C. Schindewolf, K.G. Lokugamage, D. Scharton, J.A. Plante, D. Mirchandani, S.G. Widen, K. Narayanan, S. Makino, T.G. Ksiazek, K.S. Plante, S.C. Weaver, S. Lindstrom, S. Tong, V.D. Menachery, and N.J. Thornburg, *Severe Acute Respiratory Syndrome Coronavirus 2 from Patient with Coronavirus Disease, United States.* Emerg Infect Dis, 2020. **26**(6): p. 1266-1273 DOI: 10.3201/eid2606.200516.

43. Korber, B., W.M. Fischer, S. Gnanakaran, H. Yoon, J. Theiler, W. Abfalterer, N. Hengartner, E.E. Giorgi, T. Bhattacharya, B. Foley, K.M. Hastie, M.D. Parker, D.G. Partridge, C.M. Evans, T.M. Freeman, T.I. de Silva, C.-G.G. Sheffield, C. McDanal, L.G. Perez, H. Tang, A. Moon-Walker, S.P. Whelan, C.C. LaBranche, E.O. Saphire, and D.C. Montefiori, *Tracking Changes in SARS-CoV-2 Spike: Evidence that D614G Increases Infectivity of the COVID-19 Virus.* Cell, 2020. **182**(4): p. 812-827 e19 DOI: 10.1016/j.cell.2020.06.043.

44. Andrew Rambaut, N.L., Oliver Pybus, Wendy Barclay, Jeff Barrett, Alesandro Carabelli, Tom Connor, Tom Peacock, David L Robertson, Erik Volz, on behalf of COVID-19 Genomics Consortium UK (CoG-UK), *Preliminary genomic characterisation of an emergent SARS-CoV-2 lineage in the UK defined by a novel set of spike mutations.* Virological, 2020. **Dec. 2020**.

45. O'Toole, A., V. Hill, O.G. Pybus, A. Watts, Bogoch, II, K. Khan, J.P. Messina, C.-G.U. consortium, A. Network for Genomic Surveillance in South, U.K.C.G.N. Brazil, H. Tegally, R.R. Lessells, J. Giandhari, S. Pillay, K.A. Tumedi, G. Nyepetsi, M. Kebabonye, M. Matsheka, M. Mine, S. Tokajian, H. Hassan, T. Salloum, G. Merhi, J. Koweyes, J.L. Geoghegan, J. de Ligt, X. Ren, M. Storey, N.E. Freed, C. Pattabiraman, P. Prasad, A.S. Desai, R. Vasanthapuram, T.F. Schulz, L. Steinbruck, T. Stadler, C. Swiss Viollier Sequencing, A. Parisi, A. Bianco, D. Garcia de Viedma, S. Buenestado-Serrano, V. Borges, J. Isidro, S. Duarte, J.P. Gomes, N.S. Zuckerman, M. Mandelboim, O. Mor, T. Seemann, A. Arnott, J. Draper, M. Gall, W. Rawlinson, I. Deveson, S. Schlebusch, J. McMahon, L. Leong, C.K. Lim, M. Chironna, D. Loconsole, A. Bal, L. Josset, E. Holmes, K. St George, E. Lasek-Nesselquist, R.S. Sikkema, B. Oude Munnink, M. Koopmans, M. Brytting, V. Sudha Rani, S. Pavani, T. Smura, A. Heim, S. Kurkela, M. Umair, M. Salman, B. Bartolini, M. Rueca, C. Drosten, T. Wolff, O. Silander, D. Eggink, C. Reusken, H. Vennema, A. Park, C. Carrington, N. Sahadeo, M. Carr, G. Gonzalez, S.A.S. Diego, L. National Virus Reference, C.S. Seq, C. Danish Covid-19 Genome, N. Communicable Diseases Genomic, S.-C.-s.p. Dutch National, D. Division of Emerging Infectious, T. de Oliveira, N. Faria, A. Rambaut, and M.U.G. Kraemer, *Tracking the international spread of SARS-CoV-2 lineages B.1.1.7 and B.1.351/501Y-V2 with grinch.* Wellcome Open Res, 2021. **6**: p. 121 DOI: 10.12688/wellcomeopenres.16661.2.

46. Dhar, M.S., R. Marwal, R. Vs, K. Ponnusamy, B. Jolly, R.C. Bhoyar, V. Sardana, S. Naushin, M. Rophina, T.A. Mellan, S. Mishra, C. Whittaker, S. Fatihi, M. Datta, P. Singh, U. Sharma, R. Ujjainiya, N. Bhatheja, M.K. Divakar, M.K. Singh, M. Imran, V. Senthivel, R. Maurya, N. Jha, P. Mehta, V. A, P. Sharma, A. Vr, U. Chaudhary, N. Soni, L. Thukral, S. Flaxman, S. Bhatt, R. Pandey, D. Dash, M. Faruq, H. Lall, H. Gogia, P. Madan, S. Kulkarni, H. Chauhan, S. Sengupta, S. Kabra, S.-C.-G.C.d.d. Indian, R.K. Gupta, S.K. Singh, A. Agrawal, P. Rakshit, V. Nandicoori, K.B. Tallapaka, D.T. Sowpati, K. Thangaraj, M.D. Bashyam, A. Dalal, S. Sivasubbu, V. Scaria, A. Parida, S.K. Raghav, P. Prasad, A. Sarin, S. Mayor, U. Ramakrishnan, D. Palakodeti, A.S.N. Seshasayee, M. Bhat, Y. Shouche, A. Pillai, T. Dikid, S. Das, A. Maitra, S. Chinnaswamy, N.K. Biswas, A.S. Desai, C. Pattabiraman, M.V. Manjunatha, R.S. Mani, G. Arunachal Udupi, P. Abraham, P.V. Atul, and S.S. Cherian, *Genomic characterization and epidemiology of an emerging SARS-CoV-2 variant in Delhi, India.* Science, 2021. **374**(6570): p. 995-999 DOI: 10.1126/science.abj9932.

47. Neerukonda, S.N., R. Vassell, S. Lusvarghi, R. Wang, F. Echegaray, L. Bentley, A.E. Eakin, K.J. Erlandson, L.C. Katzelnick, C.D. Weiss, and W. Wang, *SARS-CoV-2 Delta Variant Displays Moderate Resistance to Neutralizing Antibodies and Spike Protein Properties of Higher Soluble ACE2 Sensitivity, Enhanced Cleavage and Fusogenic Activity.* Viruses, 2021. **13**(12) DOI: 10.3390/v13122485.

48. Hong, Q., W. Han, J. Li, S. Xu, Y. Wang, C. Xu, Z. Li, Y. Wang, C. Zhang, Z. Huang, and Y. Cong, *Molecular basis of receptor binding and antibody neutralization of Omicron.* Nature, 2022 DOI: 10.1038/s41586-022-04581-9.

49. Smither, S.J., L.S. Eastaugh, J.S. Findlay, and M.S. Lever, *Experimental aerosol survival of SARS-CoV-2 in artificial saliva and tissue culture media at medium and high humidity.* Emerg Microbes Infect, 2020. **9**(1): p. 1415-1417 DOI: 10.1080/22221751.2020.1777906.

50. *WHO Coronavirus (COVID-19) Dashboard*. 2022 5:18pm CET, 4 March 2022; Available from: https://covid19.who.int/.

51. Rochman, N.D., Y.I. Wolf, G. Faure, P. Mutz, F. Zhang, and E.V. Koonin, *Ongoing global and regional adaptive evolution of SARS-CoV-2.* Proc Natl Acad Sci U S A, 2021. **118**(29) DOI: 10.1073/pnas.2104241118.

52. Hadfield, J., C. Megill, S.M. Bell, J. Huddleston, B. Potter, C. Callender, P. Sagulenko, T. Bedford, and R.A. Neher, *Nextstrain: real-time tracking of pathogen evolution.* Bioinformatics, 2018. **34**(23): p. 4121-4123 DOI: 10.1093/bioinformatics/bty407.

53. Konings, F., M.D. Perkins, J.H. Kuhn, M.J. Pallen, E.J. Alm, B.N. Archer, A. Barakat, T. Bedford, J.N. Bhiman, L. Caly, L.L. Carter, A. Cullinane, T. de Oliveira, J. Druce, I. El Masry, R. Evans, G.F. Gao, A.E. Gorbalenya, E. Hamblion, B.L. Herring, E. Hodcroft, E.C. Holmes, M. Kakkar, S. Khare, M.P.G. Koopmans, B. Korber, J. Leite, D. MacCannell, M. Marklewitz, S. Maurer-Stroh, J.A.M. Rico, V.J. Munster, R. Neher, B.O. Munnink, B.I. Pavlin, M. Peiris, L. Poon, O. Pybus, A. Rambaut, P. Resende, L. Subissi, V. Thiel, S. Tong, S. van der Werf, A. von Gottberg, J. Ziebuhr, and M.D. Van Kerkhove, *SARS-CoV-2 Variants of Interest and Concern naming scheme conducive for global discourse.* Nat Microbiol, 2021. **6**(7): p. 821-823 DOI: 10.1038/s41564-021-00932-w.

54. Tao, K., P.L. Tzou, J. Nouhin, R.K. Gupta, T. de Oliveira, S.L. Kosakovsky Pond, D. Fera, and R.W. Shafer, *The biological and clinical significance of emerging SARS-CoV-2 variants.* Nat Rev Genet, 2021. **22**(12): p. 757-773 DOI: 10.1038/s41576-021-00408-x.

55. Harvey, W.T., A.M. Carabelli, B. Jackson, R.K. Gupta, E.C. Thomson, E.M. Harrison, C. Ludden, R. Reeve, A. Rambaut, C.-G.U. Consortium, S.J. Peacock, and D.L. Robertson, *SARS-CoV-2 variants, spike mutations and immune escape.* Nat Rev Microbiol, 2021. **19**(7): p. 409-424 DOI: 10.1038/s41579-021-00573-0.

56. Chen, J. and G.W. Wei, *Omicron BA.2 (B.1.1.529.2): high potential to becoming the next dominating variant.* Res Sq, 2022 DOI: 10.21203/rs.3.rs-1362445/v1.

57. Grabowski, F., M. Kochanczyk, and T. Lipniacki, *The Spread of SARS-CoV-2 Variant Omicron with a Doubling Time of 2.0-3.3 Days Can Be Explained by Immune Evasion.* Viruses, 2022. **14**(2) DOI: 10.3390/v14020294.

58. Scheuch, G., *Breathing Is Enough: For the Spread of Influenza Virus and SARS-CoV-2 by Breathing Only.* J Aerosol Med Pulm Drug Deliv, 2020. **33**(4): p. 230-234 DOI: 10.1089/jamp.2020.1616.

59. Qing, E., T. Kicmal, B. Kumar, G.M. Hawkins, E. Timm, S. Perlman, and T. Gallagher, *Dynamics of SARS-CoV-2 Spike Proteins in Cell Entry: Control Elements in the Amino-Terminal Domains.* mBio, 2021. **12**(4): p. e0159021 DOI: 10.1128/mBio.01590-21.

60. Yurkovetskiy, L., X. Wang, K.E. Pascal, C. Tomkins-Tinch, T.P. Nyalile, Y. Wang, A. Baum, W.E. Diehl, A. Dauphin, C. Carbone, K. Veinotte, S.B. Egri, S.F. Schaffner, J.E. Lemieux, J.B. Munro, A. Rafique, A. Barve, P.C. Sabeti, C.A. Kyratsous, N.V. Dudkina, K. Shen, and J. Luban, *Structural and Functional Analysis of the D614G SARS-CoV-2 Spike Protein Variant.* Cell, 2020. **183**(3): p. 739-751 e8 DOI: 10.1016/j.cell.2020.09.032.

61. Zhang, J., Y. Cai, T. Xiao, J. Lu, H. Peng, S.M. Sterling, R.M. Walsh, Jr., S. Rits-Volloch, H. Zhu, A.N. Woosley, W. Yang, P. Sliz, and B. Chen, *Structural impact on SARS-CoV-2 spike protein by D614G substitution.* Science, 2021. **372**(6541): p. 525-530 DOI: 10.1126/science.abf2303.

62. Vardhan, S. and S.K. Sahoo, *Computational studies on the interaction of SARS-CoV-2 Omicron SGp RBD with human receptor ACE2, limonin and glycyrrhizic acid.* Comput Biol Med, 2022. **144**: p. 105367 DOI: 10.1016/j.compbiomed.2022.105367.

63. Jones, T.C., G. Biele, B. Muhlemann, T. Veith, J. Schneider, J. Beheim-Schwarzbach, T. Bleicker, J. Tesch, M.L. Schmidt, L.E. Sander, F. Kurth, P. Menzel, R. Schwarzer, M. Zuchowski, J. Hofmann, A. Krumbholz, A. Stein, A. Edelmann, V.M. Corman, and C. Drosten, *Estimating infectiousness throughout SARS-CoV-2 infection course.* Science, 2021. **373**(6551) DOI: 10.1126/science.abi5273.

64. van Doremalen, N., J.E. Schulz, D.R. Adney, T.A. Saturday, R.J. Fischer, C.K. Yinda, N. Thakur, J. Newman, M. Ulaszewska, S. Belij-Rammerstorfer, G. Saturday, A.J. Spencer, D. Bailey, S.C. Gilbert, T. Lambe, and V.J. Munster, *Efficacy of ChAdOx1 vaccines against SARS-CoV-2 Variants of Concern Beta, Delta and Omicron in the Syrian hamster model.* Res Sq, 2022 DOI: 10.21203/rs.3.rs-1343927/v1.

65. Letko, M., A. Marzi, and V. Munster, *Functional assessment of cell entry and receptor usage for SARS-CoV-2 and other lineage B betacoronaviruses.* Nat Microbiol, 2020. **5**(4): p. 562-569 DOI: 10.1038/s41564-020-0688-y.

66. Hu, B., H. Guo, P. Zhou, and Z.L. Shi, *Author Correction: Characteristics of SARS-CoV-2 and COVID-19.* Nat Rev Microbiol, 2022 DOI: 10.1038/s41579-022-00711-2.

67. Zou, L., F. Ruan, M. Huang, L. Liang, H. Huang, Z. Hong, J. Yu, M. Kang, Y. Song, J. Xia, Q. Guo, T. Song, J. He, H.L. Yen, M. Peiris, and J. Wu, *SARS-CoV-2 Viral Load in Upper Respiratory Specimens of Infected Patients.* N Engl J Med, 2020. **382**(12): p. 1177-1179 DOI: 10.1056/NEJMc2001737.

68. Ma, Y., L. Wu, N. Shaw, Y. Gao, J. Wang, Y. Sun, Z. Lou, L. Yan, R. Zhang, and Z. Rao, *Structural basis and functional analysis of the SARS coronavirus nsp14-nsp10 complex.* Proc Natl Acad Sci U S A, 2015. **112**(30): p. 9436-41 DOI: 10.1073/pnas.1508686112.

69. Jackson, B., M.F. Boni, M.J. Bull, A. Colleran, R.M. Colquhoun, A.C. Darby, S. Haldenby, V. Hill, A. Lucaci, J.T. McCrone, S.M. Nicholls, A. O'Toole, N. Pacchiarini, R. Poplawski, E. Scher, F. Todd, H.J. Webster, M. Whitehead, C. Wierzbicki, C.-G.U. Consortium, N.J. Loman, T.R. Connor, D.L. Robertson, O.G. Pybus, and A. Rambaut, *Generation and transmission of interlineage recombinants in the SARS-CoV-2 pandemic.* Cell, 2021. **184**(20): p. 5179-5188 e8 DOI: 10.1016/j.cell.2021.08.014.

70. Boni, M.F., P. Lemey, X. Jiang, T.T. Lam, B.W. Perry, T.A. Castoe, A. Rambaut, and D.L. Robertson, *Evolutionary origins of the SARS-CoV-2 sarbecovirus lineage*

responsible for the COVID-19 pandemic. Nat Microbiol, 2020. **5**(11): p. 1408-1417 DOI: 10.1038/s41564-020-0771-4.

71. Li, F., *Structure, Function, and Evolution of Coronavirus Spike Proteins.* Annu Rev Virol, 2016. **3**(1): p. 237-261 DOI: 10.1146/annurev-virology-110615-042301.

72. Tang, T., M. Bidon, J.A. Jaimes, G.R. Whittaker, and S. Daniel, *Coronavirus membrane fusion mechanism offers a potential target for antiviral development.* Antiviral Res, 2020. **178**: p. 104792 DOI: 10.1016/j.antiviral.2020.104792.

73. Heald-Sargent, T. and T. Gallagher, *Ready, set, fuse! The coronavirus spike protein and acquisition of fusion competence.* Viruses, 2012. **4**(4): p. 557-80 DOI: 10.3390/v4040557.

74. Saito, A., T. Irie, R. Suzuki, T. Maemura, H. Nasser, K. Uriu, Y. Kosugi, K. Shirakawa, K. Sadamasu, I. Kimura, J. Ito, J. Wu, K. Iwatsuki-Horimoto, M. Ito, S. Yamayoshi, S. Loeber, M. Tsuda, L. Wang, S. Ozono, E.P. Butlertanaka, Y.L. Tanaka, R. Shimizu, K. Shimizu, K. Yoshimatsu, R. Kawabata, T. Sakaguchi, K. Tokunaga, I. Yoshida, H. Asakura, M. Nagashima, Y. Kazuma, R. Nomura, Y. Horisawa, K. Yoshimura, A. Takaori-Kondo, M. Imai, C. Genotype to Phenotype Japan, S. Tanaka, S. Nakagawa, T. Ikeda, T. Fukuhara, Y. Kawaoka, and K. Sato, *Enhanced fusogenicity and pathogenicity of SARS-CoV-2 Delta P681R mutation.* Nature, 2022. **602**(7896): p. 300-306 DOI: 10.1038/s41586-021-04266-9.

75. Suzuki, R., D. Yamasoba, I. Kimura, L. Wang, M. Kishimoto, J. Ito, Y. Morioka, N. Nao, H. Nasser, K. Uriu, Y. Kosugi, M. Tsuda, Y. Orba, M. Sasaki, R. Shimizu, R. Kawabata, K. Yoshimatsu, H. Asakura, M. Nagashima, K. Sadamasu, K. Yoshimura, C. Genotype to Phenotype Japan, H. Sawa, T. Ikeda, T. Irie, K. Matsuno, S. Tanaka, T. Fukuhara, and K. Sato, *Attenuated fusogenicity and pathogenicity of SARS-CoV-2 Omicron variant.* Nature, 2022 DOI: 10.1038/s41586-022-04462-1.

76. Meng, B., A. Abdullahi, I. Ferreira, N. Goonawardane, A. Saito, I. Kimura, D. Yamasoba, P.P. Gerber, S. Fatihi, S. Rathore, S.K. Zepeda, G. Papa, S.A. Kemp, T. Ikeda, M. Toyoda, T.S. Tan, J. Kuramochi, S. Mitsunaga, T. Ueno, K. Shirakawa, A. Takaori-Kondo, T. Brevini, D.L. Mallery, O.J. Charles, C.-N.B.C.-. Collaboration, C. Genotype to Phenotype Japan, C.C. Ecuador, J.E. Bowen, A. Joshi, A.C. Walls, L. Jackson, D. Martin, K.G.C. Smith, J. Bradley, J.A.G. Briggs, J. Choi, E. Madissoon, K.B. Meyer, P. Mlcochova, L. Ceron-Gutierrez, R. Doffinger, S.A. Teichmann, A.J. Fisher, M.S. Pizzuto, A. de Marco, D. Corti, M. Hosmillo, J.H. Lee, L.C. James, L. Thukral, D. Veesler, A. Sigal, F. Sampaziotis, I.G. Goodfellow, N.J. Matheson, K. Sato, and R.K.

Gupta, *Altered TMPRSS2 usage by SARS-CoV-2 Omicron impacts infectivity and fusogenicity.* Nature, 2022. **603**(7902): p. 706-714 DOI: 10.1038/s41586-022-04474-x.

77. Liu, Y., J. Liu, B.A. Johnson, H. Xia, Z. Ku, C. Schindewolf, S.G. Widen, Z. An, S.C. Weaver, V.D. Menachery, X. Xie, and P.Y. Shi, *Delta spike P681R mutation enhances SARS-CoV-2 fitness over Alpha variant.* bioRxiv, 2021 DOI: 10.1101/2021.08.12.456173.

78. Burki, T.K., *Omicron variant and booster COVID-19 vaccines.* Lancet Respir Med, 2022. **10**(2): p. e17 DOI: 10.1016/S2213-2600(21)00559-2.

79. Rossmann, M.G., *The canyon hypothesis. Hiding the host cell receptor attachment site on a viral surface from immune surveillance.* J Biol Chem, 1989. **264**(25): p. 14587-90.

80. *Science Brief: SARS-CoV-2 and Surface (Fomite) Transmission for Indoor Community Environments*, in *CDC COVID-19 Science Briefs*. 2020: Atlanta (GA).

81. Rocha, A.L.S., J.R. Pinheiro, T.C. Nakamura, J.D.S. da Silva, B.G.S. Rocha, R.C. Klein, A. Birbrair, and J.H. Amorim, *Fomites and the environment did not have an important role in COVID-19 transmission in a Brazilian mid-sized city.* Sci Rep, 2021. **11**(1): p. 15960 DOI: 10.1038/s41598-021-95479-5.

82. Ryohei Hirose, Y.I., Hiroshi Ikegaya, Hajime Miyazaki, Naoto Watanabe, Takuma Yoshida, Risa Bandou, Tomo Daidoji, Takaaki Nakaya, *Differences in environmental stability among SARS-CoV-2 variants of concern: Omicron has higher stability.* bioRxiv, 2022 DOI: https://doi.org/10.1101/2022.01.18.476607.

83. Arora, P., L. Zhang, C. Rocha, A. Sidarovich, A. Kempf, S. Schulz, A. Cossmann, B. Manger, E. Baier, B. Tampe, O. Moerer, S. Dickel, A. Dopfer-Jablonka, H.M. Jack, G.M.N. Behrens, M.S. Winkler, S. Pohlmann, and M. Hoffmann, *Comparable neutralisation evasion of SARS-CoV-2 omicron subvariants BA.1, BA.2, and BA.3.* Lancet Infect Dis, 2022 DOI: 10.1016/S1473-3099(22)00224-9.

84. Frederik Plesner Lyngse, C.T.K., Matthew Denwood, Lasse Engbo Christiansen, Kåre Mølbak, Camilla Holten Møller, Robert Leo Skov, Tyra Grove Krause, Morten Rasmussen, Raphael Niklaus Sieber, Thor Bech Johannesen, Troels Lillebaek, Jannik Fonager, Anders Fomsgaard, Frederik Trier Møller, Marc Stegger, Maria Overvad, Katja Spiess, Laust Hvas Mortensen, *Transmission of SARS-CoV-2 Omicron VOC subvariants BA.1 and BA.2: Evidence from Danish Households.* medRxiv, 2022.

85. Olha Puhach, K.A., Nicolas Hulo, Pascale Sattonnet, Camille Genecand, Anne Iten, Frédérique Jacquérioz Bausch, Laurent Kaiser, Pauline Vetter, Isabella Eckerle, Benjamin Meyer, *Infectious viral load in unvaccinated and vaccinated patients infected with SARS-CoV-2 WT, Delta and Omicron.* MedRxiv, 2022 DOI: https://doi.org/10.1101/2022.01.10.22269010.

86. James A. Hay, V.O.P.M.K., Joseph R. Fauver, Christina Mack, Caroline G. Tai, Radhika M. Samant, Sarah Connelly, Deverick J. Anderson, Gaurav Khullar, Matthew MacKay, Miral Patel, Shannan Kelly, April Manhertz, Isaac Eiter, Daisy Salgado, Tim Baker, Ben Howard, Joel T. Dudley, Christopher E. Mason, David D. Ho, Nathan D. Grubaugh, Yonatan H. Grad, *Viral dynamics and duration of PCR positivity of the SARS-CoV-2 Omicron variant.* medRxiv, 2022 DOI: https://doi.org/10.1101/2022.01.13.22269257.

87. McCallum, M., N. Czudnochowski, L.E. Rosen, S.K. Zepeda, J.E. Bowen, A.C. Walls, K. Hauser, A. Joshi, C. Stewart, J.R. Dillen, A.E. Powell, T.I. Croll, J. Nix, H.W. Virgin, D. Corti, G. Snell, and D. Veesler, *Structural basis of SARS-CoV-2 Omicron immune evasion and receptor engagement.* Science, 2022. **375**(6583): p. 864-868 DOI: 10.1126/science.abn8652.

88. *ProMED-mail post.* 2022 28 April 2022; Available from: https://promedmail.org/.

89. van Doremalen, N., T. Bushmaker, D.H. Morris, M.G. Holbrook, A. Gamble, B.N. Williamson, A. Tamin, J.L. Harcourt, N.J. Thornburg, S.I. Gerber, J.O. Lloyd-Smith, E. de Wit, and V.J. Munster, *Aerosol and surface stability of HCoV-19 (SARS-CoV-2) compared to SARS-CoV-1.* medRxiv, 2020 DOI: 10.1101/2020.03.09.20033217.

90. Fischer, R.J., D.H. Morris, N. van Doremalen, S. Sarchette, M.J. Matson, T. Bushmaker, C.K. Yinda, S.N. Seifert, A. Gamble, B.N. Williamson, S.D. Judson, E. de Wit, J.O. Lloyd-Smith, and V.J. Munster, *Assessment of N95 respirator decontamination and re-use for SARS-CoV-2.* medRxiv, 2020 DOI: 10.1101/2020.04.11.20062018.

91. van Doremalen, N., T. Lambe, A. Spencer, S. Belij-Rammerstorfer, J.N. Purushotham, J.R. Port, V. Avanzato, T. Bushmaker, A. Flaxman, M. Ulaszewska, F. Feldmann, E.R. Allen, H. Sharpe, J. Schulz, M. Holbrook, A. Okumura, K. Meade-White, L. Perez-Perez, C. Bissett, C. Gilbride, B.N. Williamson, R. Rosenke, D. Long, A. Ishwarbhai, R. Kailath, L. Rose, S. Morris, C. Powers, J. Lovaglio, P.W. Hanley, D. Scott, G. Saturday, E. de Wit, S.C. Gilbert, and V.J. Munster, *ChAdOx1 nCoV-19 vaccination prevents SARS-CoV-2 pneumonia in rhesus macaques.* bioRxiv, 2020 DOI: 10.1101/2020.05.13.093195.

92. Yinda, C.K., J.R. Port, T. Bushmaker, I. Offei Owusu, J.N. Purushotham, V.A. Avanzato, R.J. Fischer, J.E. Schulz, M.G. Holbrook, M.J. Hebner, R. Rosenke, T. Thomas, A. Marzi, S.M. Best, E. de Wit, C. Shaia, N. van Doremalen, and V.J. Munster, *K18-hACE2 mice develop respiratory disease resembling severe COVID-19*. PLoS Pathog, 2021. **17**(1): p. e1009195 DOI: 10.1371/journal.ppat.1009195.

93. van Doremalen, N., J.N. Purushotham, J.E. Schulz, M.G. Holbrook, T. Bushmaker, A. Carmody, J.R. Port, C.K. Yinda, A. Okumura, G. Saturday, F. Amanat, F. Krammer, P.W. Hanley, B.J. Smith, J. Lovaglio, S.L. Anzick, K. Barbian, C. Martens, S.C. Gilbert, T. Lambe, and V.J. Munster, *Intranasal ChAdOx1 nCoV-19/AZD1222 vaccination reduces viral shedding after SARS-CoV-2 D614G challenge in preclinical models.* Sci Transl Med, 2021. **13**(607) DOI: 10.1126/scitranslmed.abh0755.

94. Morris, D.H., K.C. Yinda, A. Gamble, F.W. Rossine, Q. Huang, T. Bushmaker, R.J. Fischer, M.J. Matson, N. Van Doremalen, P.J. Vikesland, L.C. Marr, V.J. Munster, and J.O. Lloyd-Smith, *Mechanistic theory predicts the effects of temperature and humidity on inactivation of SARS-CoV-2 and other enveloped viruses.* Elife, 2021. **10** DOI: 10.7554/eLife.65902.

95. Shapira, T., I.A. Monreal, S.P. Dion, D.W. Buchholz, B. Imbiakha, A.D. Olmstead, M. Jager, A. Desilets, G. Gao, M. Martins, T. Vandal, C.A.H. Thompson, A. Chin, W.D. Rees, T. Steiner, I.R. Nabi, E. Marsault, J. Sahler, D.G. Diel, G.R. Van de Walle, A. August, G.R. Whittaker, P.L. Boudreault, R. Leduc, H.C. Aguilar, and F. Jean, *A TMPRSS2 inhibitor acts as a pan-SARS-CoV-2 prophylactic and therapeutic.* Nature, 2022 DOI: 10.1038/s41586-022-04661-w.